Article

Global and regional drivers of land-use emissions in 1961–2017

https://doi.org/10.1038/s41586-020-03138-y

Received: 26 November 2019

Accepted: 23 October 2020

Published online: 27 January 2021

Check for updates

Chaopeng Hong[1]✉, Jennifer A. Burney[2]✉, Julia Pongratz[3,4], Julia E. M. S. Nabel[4], Nathaniel D. Mueller[5,6], Robert B. Jackson[7,8,9] & Steven J. Davis[1,10]✉

Historically, human uses of land have transformed and fragmented ecosystems[1,2], degraded biodiversity[3,4], disrupted carbon and nitrogen cycles[5,6] and added prodigious quantities of greenhouse gases (GHGs) to the atmosphere[7,8]. However, in contrast to fossil-fuel carbon dioxide (CO_2) emissions, trends and drivers of GHG emissions from land management and land-use change (together referred to as 'land-use emissions') have not been as comprehensively and systematically assessed. Here we present country-, process-, GHG- and product-specific inventories of global land-use emissions from 1961 to 2017, we decompose key demographic, economic and technical drivers of emissions and we assess the uncertainties and the sensitivity of results to different accounting assumptions. Despite steady increases in population (+144 per cent) and agricultural production per capita (+58 per cent), as well as smaller increases in emissions per land area used (+8 per cent), decreases in land required per unit of agricultural production (−70 per cent) kept global annual land-use emissions relatively constant at about 11 gigatonnes CO_2-equivalent until 2001. After 2001, driven by rising emissions per land area, emissions increased by 2.4 gigatonnes CO_2-equivalent per decade to 14.6 gigatonnes CO_2-equivalent in 2017 (about 25 per cent of total anthropogenic GHG emissions). Although emissions intensity decreased in all regions, large differences across regions persist over time. The three highest-emitting regions (Latin America, Southeast Asia and sub-Saharan Africa) dominate global emissions growth from 1961 to 2017, driven by rapid and extensive growth of agricultural production and related land-use change. In addition, disproportionate emissions are related to certain products: beef and a few other red meats supply only 1 per cent of calories worldwide, but account for 25 per cent of all land-use emissions. Even where land-use change emissions are negligible or negative, total per capita CO_2-equivalent land-use emissions remain near 0.5 tonnes per capita, suggesting the current frontier of mitigation efforts. Our results are consistent with existing knowledge—for example, on the role of population and economic growth and dietary choice—but provide additional insight into regional and sectoral trends.

Stabilizing global mean temperature at levels below 2 °C requires near-zero emissions of longer-lived GHGs such as CO_2 and N_2O by mid-century[9,10], although the timeline to zero may be extended somewhat by reductions in emissions of shorter-lived CH_4 (refs. [11,12]). The Paris Agreement also sets an ambitious goal "to achieve a balance between anthropogenic emissions by sources and removals by sinks of greenhouse gases in the second half of this century". To these ends, trends in countries' fossil fuel CO_2 emissions are fastidiously tracked and routinely decomposed into drivers of population and economic growth, the energy intensity of economic activity, and the carbon intensity of energy production to enable evaluation and prioritization of climate mitigation efforts[13,14]. By contrast, although agricultural production (including both crops and livestock) and land-use change are also major sources of GHG emissions[15,16], trends in such land-use emissions and changes in their specific sources have most often been analysed as one process or product in one region at a time[17–20]. Although a few studies explored drivers of land-use changes and related emissions[21–23], none systematically investigate and decompose the drivers of all land-use emissions across different process sources, spatial scales (global, regional and national) and products.

[1]Department of Earth System Science, University of California, Irvine, Irvine, CA, USA. [2]School of Global Policy and Strategy, University of California, San Diego, San Diego, CA, USA. [3]Department of Geography, Ludwig-Maximilians-Universität, Munich, Germany. [4]Department of Land in the Earth System, Max Planck Institute for Meteorology, Hamburg, Germany. [5]Department of Ecosystem Science and Sustainability, Colorado State University, Fort Collins, CO, USA. [6]Department of Soil and Crop Sciences, Colorado State University, Fort Collins, CO, USA. [7]Department of Earth System Science, Stanford University, Stanford, CA, USA. [8]Woods Institute for the Environment, Stanford University, Stanford, CA, USA. [9]Precourt Institute for Energy, Stanford University, Stanford, CA, USA. [10]Department of Civil and Environmental Engineering, University of California, Irvine, Irvine, CA, USA. ✉e-mail: hcp12@tsinghua.org.cn; jburney@ucsd.edu; sjdavis@uci.edu

Compared to fossil fuel CO_2 emissions, land-use emissions are difficult to assess: they are spatially diffuse (that is, area—as opposed to point—sources), temporally distributed (for example, emissions from a deforested area may occur over many years) and require substantially more data and disciplinary knowledge to estimate (for example, detailed data on changes in land cover and agronomic practices, and understanding of complex biogeochemical processes)[24,25]. Land-use emissions may also be comparatively difficult to avoid: emission-free (or net-zero) alternatives for large-scale food production do not currently exist. Moreover, in addition to land use being a source of emissions, land management may be an important mechanism for CO_2 removal (that is, negative emissions) in the future[26]. Prioritizing opportunities to avoid land-use emissions (or increase negative emissions) will depend upon quantifying differences in the magnitude, intensity and drivers of such emissions across regions, processes and products.

Here, we present the results of a country-level analysis of trends in global land-use emissions in 1961–2017 and their demographic, economic and technical drivers. Details of our analytic approach and accounting assumptions are described in Methods. In summary, we use annual time-series data on population, crop and livestock production, land area harvested and agricultural emissions[15], as well as spatially explicit data on land-use change emissions[24], to estimate and attribute global land-use emissions among 229 countries or areas, 169 agricultural products and 13 sources or processes (see Extended Data Table 1). We assign emissions to the country in which they are physically produced (that is, production-based accounting; as opposed to where related goods are consumed). Our base case also attributes emissions related to crops fed to livestock to the feed crops themselves, assigns land-use change emissions to the year in which they probably occurred, evaluates agricultural production in units of energy content (kilocalories) and estimates emissions in units of CO_2-equivalent (CO_2-eq) using 100-year Global Warming Potentials (GWP_{100}) of CH_4 and N_2O. However, we also analyse uncertainties related to input data and model parameters, test the sensitivity of our estimates to alternative metrics (for example, GWP*) and accounting conventions[24,25], and compare our results with other studies[27–29] (see Methods and Extended Data Figs. 1–7).

We assess land-use emissions from different processes and analyse the drivers of these emissions over the 57-year period using a *Pale* identity—an adaptation of the Kaya identity used for fossil fuel CO_2 emissions:

$$E = P\left(\frac{A}{P}\right)\left(\frac{L}{A}\right)\left(\frac{E}{L}\right) = Pale = Paf, \quad (1)$$

where E represents the global flux of land-use GHG emissions from all processes (excluding fossil fuel and industrial process emissions), P is the population, A is agricultural production and L is the area of agricultural land use (cropland and pasture); $a = A/P$ is the per capita production of agricultural goods, $l = L/A$ is land-use intensity of agricultural production (that is, the inverse of agricultural yield), $e = E/L$ is the emissions intensity of land use and $f = E/A = le$ is the emissions intensity of agricultural production. By this decomposition, we highlight not only the products and locations where emissions might be avoided, but the associated socioeconomic and technical leverage points.

Trends and drivers of global emissions

Figure 1 shows our base estimates of global land-use emissions in 1961–2017 broken down by regions, processes, product groups and GHGs. Net cumulative emissions over the 57-year period were 657 Gt CO_2-eq (465–744 Gt CO_2-eq under different assumptions; Extended Data Fig. 1). Land-use emissions account for 27% (68% intervals, 22–29%; see Methods) of global total anthropogenic GHG emissions in 1970–2017, with the share of annual anthropogenic GHG emissions ranging from 35% (28–36%) in 1970 to 22% (17–24%) in 2011 (25% in 2017; Table 1). Latin America, sub-Saharan Africa and Southeast Asia are consistently the largest regional sources of land-use emissions, together representing 53% (45–58%) of net cumulative emissions in 1961–2017, despite large carbon uptake due to forest regrowth in shifting cultivation in those regions (Fig. 1a). Land-use change to cropland (LUC-Crops) and enteric fermentation together represent 95% (77–109%) of global net emissions over this period, with agriculture abandonment representing nearly all carbon uptake (Fig. 1b). Similarly, cereals are the product group associated with the greatest global emissions, followed by beef, with these two together representing 71% (68–77%) of global net emissions (Fig. 1c). Finally, reflecting the importance of land-use

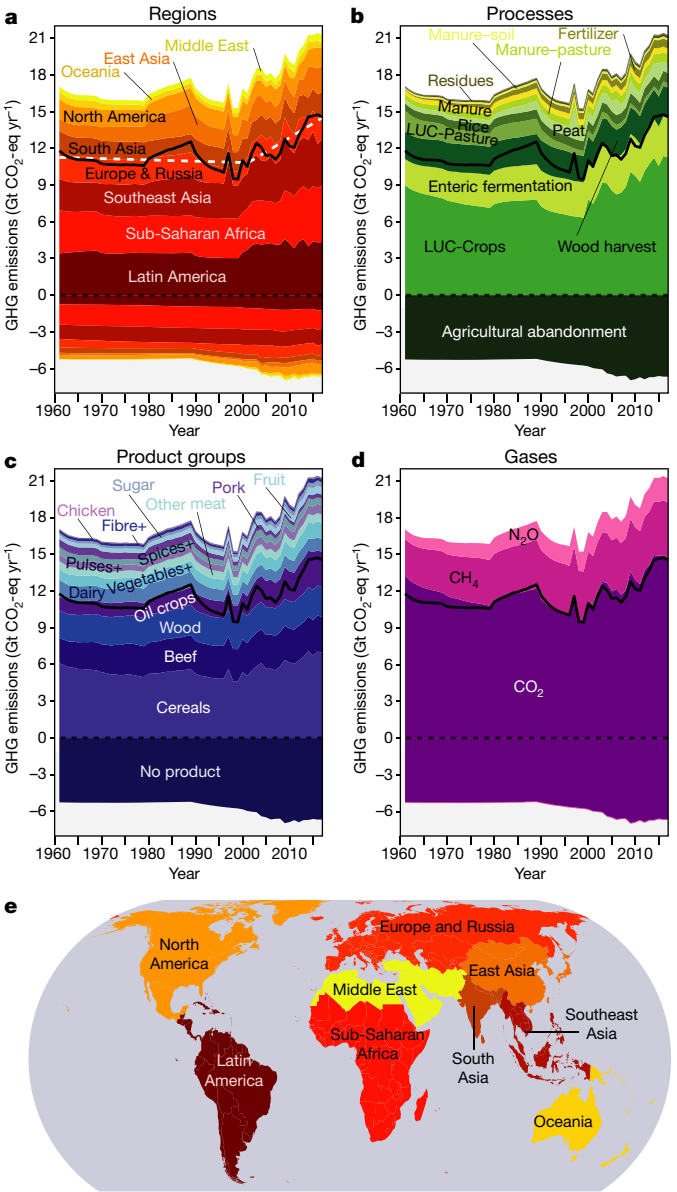

Fig. 1 | Estimated emissions from land-use change and land management (land-use emissions) over the period 1961–2017. a–d, Estimated land-use emissions by world region (**a**), process (**b**), product group (see Extended Data Table 2) (**c**) and GHG emitted (**d**). In each panel, net emissions are shown by the bold black line. The white dashed line in **a** is a piecewise linear fit of net emissions, which indicates an inflection point in 2001. **e**, Definition of the nine world regions examined in this study, shaded as in **a**. The map was made with Natural Earth free vector and raster map data (www.naturalearthdata.com) using Matlab (Mathworks, version 2017b).

Table 1 | Global land-use emissions in 2017, by product group

Product group	CO_2 (Mt yr^{-1})	CH_4 (Mt CO_2-eq yr^{-1})	N_2O (Mt CO_2-eq yr^{-1})	Land-use GHG emissions (Mt CO_2-eq yr^{-1})	Fraction of total land-use GHG emissions (%)	Fraction of total anthropogenic GHG emissions (%)
Cereals	5,480 (3,209 to 5,729)	898 (555 to 1,234)	574 (382 to 791)	6,952 (4,305 to 7,609)	47.7 (39.3 to 53.3)	11.8 (7.9 to 12.8)
Beef	76 (−42 to 180)	2,293 (1,761 to 2,818)	567 (345 to 784)	2,935 (2,254 to 3,639)	20.2 (16.5 to 30.2)	5.0 (4.0 to 6.3)
Oilcrops	2,770 (1,608 to 3,016)	–	124 (78 to 173)	2,894 (1,687 to 3,189)	19.9 (14.3 to 23.4)	4.9 (3.0 to 5.6)
Wood	2,428 (1,244 to 2,587)	–	–	2,428 (1,244 to 2,587)	16.7 (10.2 to 18.7)	4.1 (2.2 to 4.6)
Veg+	1,233 (698 to 1,288)	–	91 (55 to 132)	1,324 (753 to 1,420)	9.1 (6.5 to 10.4)	2.3 (1.3 to 2.5)
Dairy	120 (−83 to 301)	725 (558 to 882)	195 (130 to 267)	1,040 (656 to 1,402)	7.1 (4.9 to 11.8)	1.8 (1.2 to 2.5)
Pulses+	727 (404 to 803)	–	19 (11 to 26)	745 (415 to 829)	5.1 (3.5 to 6.1)	1.3 (0.7 to 1.5)
Other meat	44 (−16 to 90)	417 (321 to 512)	213 (125 to 298)	674 (484 to 851)	4.6 (3.5 to 7.2)	1.1 (0.8 to 1.5)
Fruit	552 (317 to 572)	–	41 (23 to 60)	594 (340 to 633)	4.1 (2.9 to 4.6)	1.0 (0.6 to 1.1)
Spices+	527 (322 to 585)	–	10 (6 to 15)	538 (327 to 600)	3.7 (2.7 to 4.4)	0.9 (0.6 to 1.1)
Sugar	364 (196 to 390)	2 (1 to 2)	32 (19 to 47)	398 (217 to 439)	2.7 (1.9 to 3.2)	0.7 (0.4 to 0.8)
Pork	109 (−24 to 237)	163 (125 to 200)	73 (51 to 101)	345 (171 to 523)	2.4 (1.2 to 4.3)	0.6 (0.3 to 0.9)
Fibre+	269 (165 to 288)	–	6 (3 to 8)	275 (168 to 297)	1.9 (1.4 to 2.2)	0.5 (0.3 to 0.5)
Chicken	23 (−14 to 55)	9 (7 to 12)	54 (36 to 72)	86 (32 to 137)	0.6 (0.2 to 1.2)	0.1 (0.0 to 0.2)
Total	8,061 (4,530 to 8,487)	4,507 (3,461 to 5,480)	1,999 (1,482 to 2,584)	14,567 (9,841 to 16,116)	100.0 (100.0 to 100.0)	24.8 (18.6 to 26.4)

Values are calculated using GWP_{100}. The 68% uncertainty ranges are shown in parentheses, determined by uncertainties in land-use change emissions and in agricultural emissions, as well as uncertainties in the GWP_{100} values. According to the Global Carbon Budget 2019[30], CO_2 emissions from fossil fuel and industrial sources in 2017 were 35.8 Gt. CH_4 and N_2O emissions from non-agricultural sectors in 2017 were estimated to be 7.46 Gt CO_2-eq and 0.87 Gt CO_2-eq, respectively, based on the extrapolation of 2000–2015 emissions from EDGARv5.0[28]. We note that carbon uptake from agriculture abandonment is not included in the product allocation.

change, net CO_2 emissions represent 54% (39–61%) of all GHG emissions (Fig. 1d).

In our base case, net annual emissions ranged from 9.5 to 14.7 Gt CO_2-eq yr^{-1} during 1961–2017, averaging 11.5 Gt (8.2–12.9 Gt) and reaching 14.6 Gt (9.8–16.1 Gt) in 2017, a value 24% (19–37%) greater than in 1961. The growth of net annual emissions reflects a long-term trend of agricultural intensification in which steady increases in agricultural emissions (2.7 Gt greater in 2017 than in 1961, mostly related to enteric fermentation, fertilizer, manure and rice cultivation) have been offset by changes in net land-use change emissions. The share of all land-use emissions related to agricultural processes (that is, excluding land-use change) increased from 32% (27–48%) in 1961 to 45% (38–63%) in 2017 (Fig. 2a). After 2001, the balance between increasing agricultural emissions and decreasing land-use change emissions broke down: between 2001 and 2017, net annual emissions increased at a rate of 2.4 Gt CO_2-eq per decade (Fig. 1a). This increase reflects a reversal of prior decreases in land-use change emissions (also visible in the results of dynamic global vegetation models[30]; but see estimates of emissions by Houghton and Nassikas[29], which begin to increase in the mid-1980s) and continued growth of agricultural emissions (Extended Data Fig. 8a; agricultural emissions stabilized in the 1990s and then resumed growth).

Figure 2a shows per cent changes in the drivers of global land-use emissions relative to 1961 (that is, the *Pale* factors; equation (1)). Global emissions increased by 24% (19–37%) between 1961 and 2017 (Fig. 2a), reflecting a balance between increases in population (+144%; *P*) and agricultural production per capita (+58%; 52–64%; *a*) and steady and substantial decreases in the land intensity of agricultural production (−70%; −69% to −72%; *l*). Increases in the emissions intensity of land use (+8%; 3–20%; *e*) played a lesser part in suppressing emissions, but sudden and substantial variations in this intensity nonetheless dominate interannual variability in global emissions by upsetting the rough equilibrium between increasing production and improving yields. The growth in land-use emissions after 2001 also reflects a recent increase in the emissions intensity of land use.

By further decomposing these drivers in land-use change and agricultural emissions, we find that the volatile trend in emissions per unit area of land used (and thereby emissions) is almost entirely related to substantial variations in land-use change, and particularly the rate of cropland expansion (Extended Data Fig. 8a). By contrast, the component of land-use emissions intensity related to agricultural processes increases steadily, reflecting overall increases in agricultural inputs and outputs (for example, fertilizers and manure; Extended Data Fig. 8a).

Combined, large decreases in land area per unit of total agricultural production and slight increases in emissions per unit area of land result in a 68% (63–70%) decrease in emissions per unit of agricultural production, reflecting a progressive decoupling of land-use emissions from agricultural production at the global scale mostly driven by agricultural intensification.

Trends and drivers of regional emissions

Figure 2 also shows per cent changes in the drivers of land-use emissions in each region, revealing both consistent features and profound differences. For example, population increased in all regions between 1961 and 2017, with the greatest increases in sub-Saharan Africa (+352%), the Middle East (+298%), Southeast Asia (+194%) and South Asia (+192%). Similarly, agricultural production per capita increased almost everywhere over that period, ranging from a modest +7% in the Middle East to a startling +279% in Southeast Asia). The only exception was sub-Saharan Africa, where agricultural production did not keep pace with the rapid population growth (per capita production decreased by 10%; Fig. 2d).

The land intensity of agricultural production decreased in all regions, with the greatest progress in Southeast Asia (−81%) and Latin America (−81%), and somewhat less improvement in industrialized regions such as North America (−67%), Europe and Russia (−49%; although the decline and collapse of the Soviet Union in the early 1990s is evident; Fig. 2). By contrast, regional trends in the emissions intensity of land use diverge across regions and often fluctuate over time (Fig. 2), driven primarily by substantial regional differences in land-use change (Extended Data Fig. 8).

In turn, the differences in land-use change and emissions intensity translate into large relative differences in regional land-use emissions.

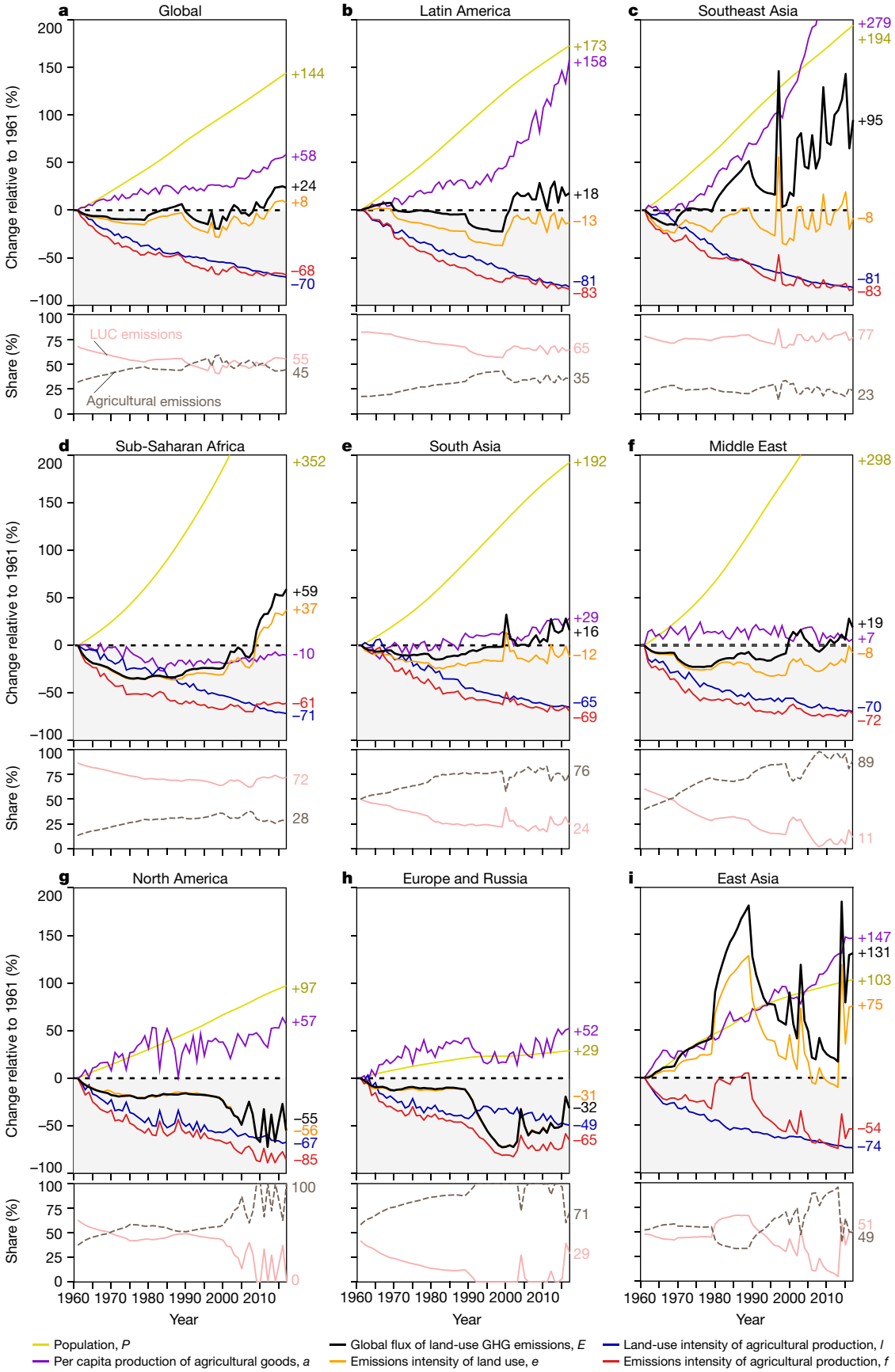

Fig. 2 | Global and regional drivers of land-use emissions in 1961–2017. **a**–**i**, Upper plots in each panel show changes over the period 1961–2017 in land-use emissions (black curves) and *Pale* factors (*P*, population; *a*, per capita production of agricultural goods; *l*, land-use intensity of agricultural production; *e*, emissions intensity of land use; *E*, global flux of land-use GHG emissions; *f*, emissions intensity of agricultural production) for the global total (**a**) and for each region (**b**–**i**) relative to 1961. Lower plots show the corresponding shares of annual land-use emissions from land-use change (LUC; pink curves) and agricultural (dashed grey curves) processes (shares are of emissions only, neglecting any carbon uptake). Oceania is not shown.

Land-use emissions declined by an average of 0.7% (0.3–0.9%) per year between 1961 and 2017 in Europe and Russia (Fig. 2h), whereas they rose by 1.2% (1.1–1.5%) per year on average in Southeast Asia over the same period (Fig. 2c). The importance of land-use change to emissions trends is recognizable by differences in the per cent changes of emissions and emissions intensity of land use: there is little difference where the area of agricultural lands is relatively stable (for example, North America, Europe and Russia), but when and where agricultural lands expand, trends in emissions mostly reflect changes in the area of land used rather than intensification and increased non-CO_2 emissions (for example, Southeast Asia, Latin America and East Asia).

The three highest-emitting regions—Latin America, Southeast Asia and sub-Saharan Africa—account for 53% of global land-use emissions and more than two-thirds of global emissions growth over the period from 1961 to 2017 (Fig. 1a). In each of these regions, sharp increases in land-use emissions are associated with cropland expansion and concomitant spikes in the emissions intensity of land use (Extended Data Fig. 8, Fig. 2b–d). In the case of Latin America, increases in emissions after 2000 reversed earlier long-term declines; emissions in this region reached roughly 75% of 1961 levels in the 1990s (but see estimates by Houghton and Nassikas[29], which increase beginning in the mid-1980s). By contrast, emissions in Southeast Asia and sub-Saharan Africa have trended upwards throughout most of that period, driven by particularly rapid and extensive growth of agricultural production (Fig. 2c, Extended Data Fig. 8c). Combined, the area of cropland in these three highest-emitting regions increased by ~160% between 1961 and 2017 (~71% of the global increase). Moreover, the CO_2 emissions per area converted in these regions were particularly large[31] and land-use change emissions account for 65–77% of their land-use emissions (Fig. 2). Another indication of extensive agricultural growth in these three regions is that they account for only 16% of global fertilizer consumption[15] but for 31% of global agricultural production since 2000.

East Asia reveals the potential for cutting emissions by controlling land-use change: Chinese land and market reforms increased land conversions and agricultural emissions in the region during the 1980s, transforming large areas of primary forests; but as the agricultural expansion stopped in the 1990s (Extended Data Fig. 8i), emissions dropped sharply (Fig. 2i), and by 2013 net emissions related to land-use change were nearly zero (Extended Data Figs. 8i, 9h; but see estimates of East Asian land-use change emissions by Houghton and Nassikas[29], which decrease throughout this period). However, such patterns may have been enabled by increases in agricultural imports during this period, which may have spurred land-use change in other regions, and land-use change emissions have increased again in the past few years owing to cropland expansion.

When and where land-use change is not a major source of land-use emissions, trends in emissions largely mirror changes in the emissions intensity of agricultural processes (*f*). For example, in South Asia and the Middle East, slow increases in emissions over the past several decades reflect increases in agricultural production but stagnation of the emissions intensity of that production, suggesting that a breakthrough may be needed to achieve large reductions. In North America, Europe and Russia, and Oceania, agricultural emissions have not changed much in recent years, but overall land-use emissions in these regions are still decreasing owing to carbon uptake by regrowing forests (Fig. 2g, h, Extended Data Figs. 8g, h, 9f, g, i).

Targeted mitigation opportunities

Figure 3 shows the geographic distribution of key *Pale* factors in 2017. Patterns of agricultural production per capita emphasize large industrialized countries and emerging markets such as the USA, Europe, Brazil, Argentina, Russia, Indonesia and Oceania, with lower productivity in countries of Africa, South Asia and the Middle East (Fig. 3a). By contrast, the emissions intensity of land use is greatest in forested countries of Latin America, sub-Saharan Africa and Southeast Asia—where conversion of carbon-dense and often still pristine, undegraded natural systems is driving the highest levels of land-use emissions (Figs. 3b, 1a). The land intensity of agricultural production is greatest in poorer and/or naturally unproductive regions in Africa and central Asia (Fig. 3c). Together, the emissions intensity of agricultural production is greatest in forested and/or land-intensive countries in Latin America, Africa, Southeast Asia and central Asia (Fig. 3d).

Figure 4 explores country- and product-level differences in greater detail, in an effort to identify specific countries and products with emissions or emissions intensities that are anomalously high and may therefore be attractive 'mitigation targets'. Of the 30 countries with the greatest overall land-use emissions, we plot the top 10 countries in 2017 for each of the *Pale* factors (Fig. 4a–f; for comparison, circles indicate values in 1961). The ten countries in Fig. 4a are the largest producers of

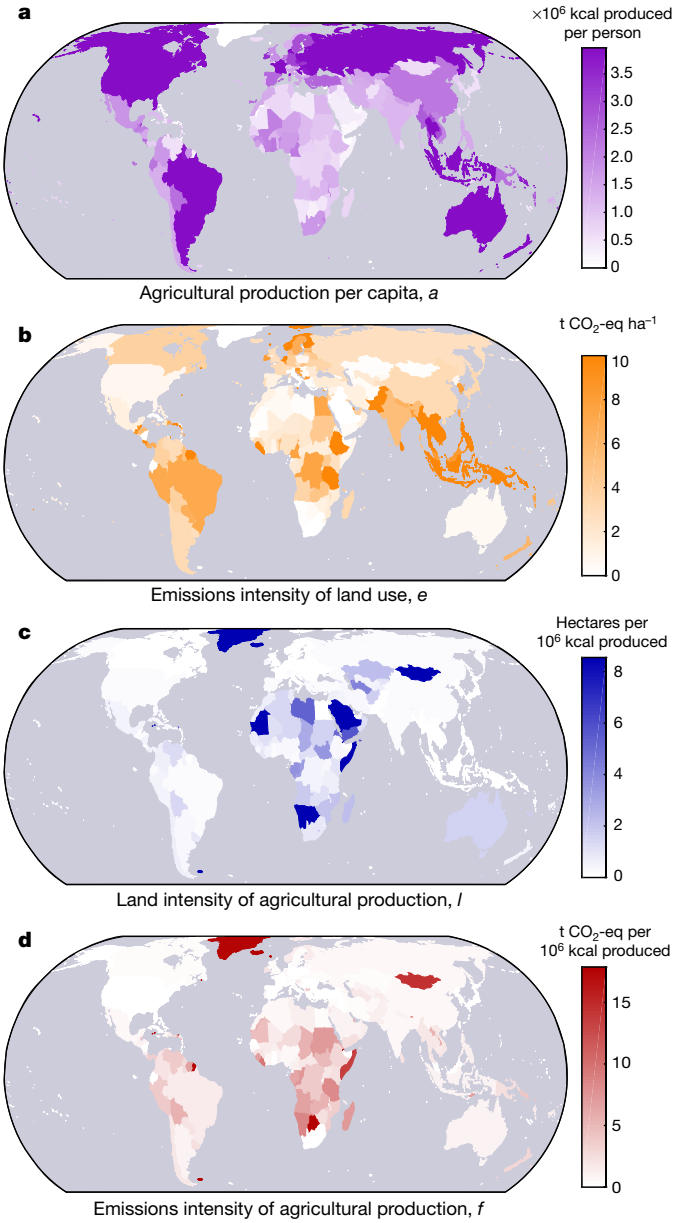

Fig. 3 | Global distribution of key *Pale* factors in 2017. a, Agricultural production per capita. **b**, Emissions intensity of land use. **c**, Land intensity of agricultural production (inverse of yield). **d**, Emissions intensity of agricultural production. The map was made with Natural Earth free vector and raster map data (www.naturalearthdata.com), using Matlab (Mathworks, version 2017b).

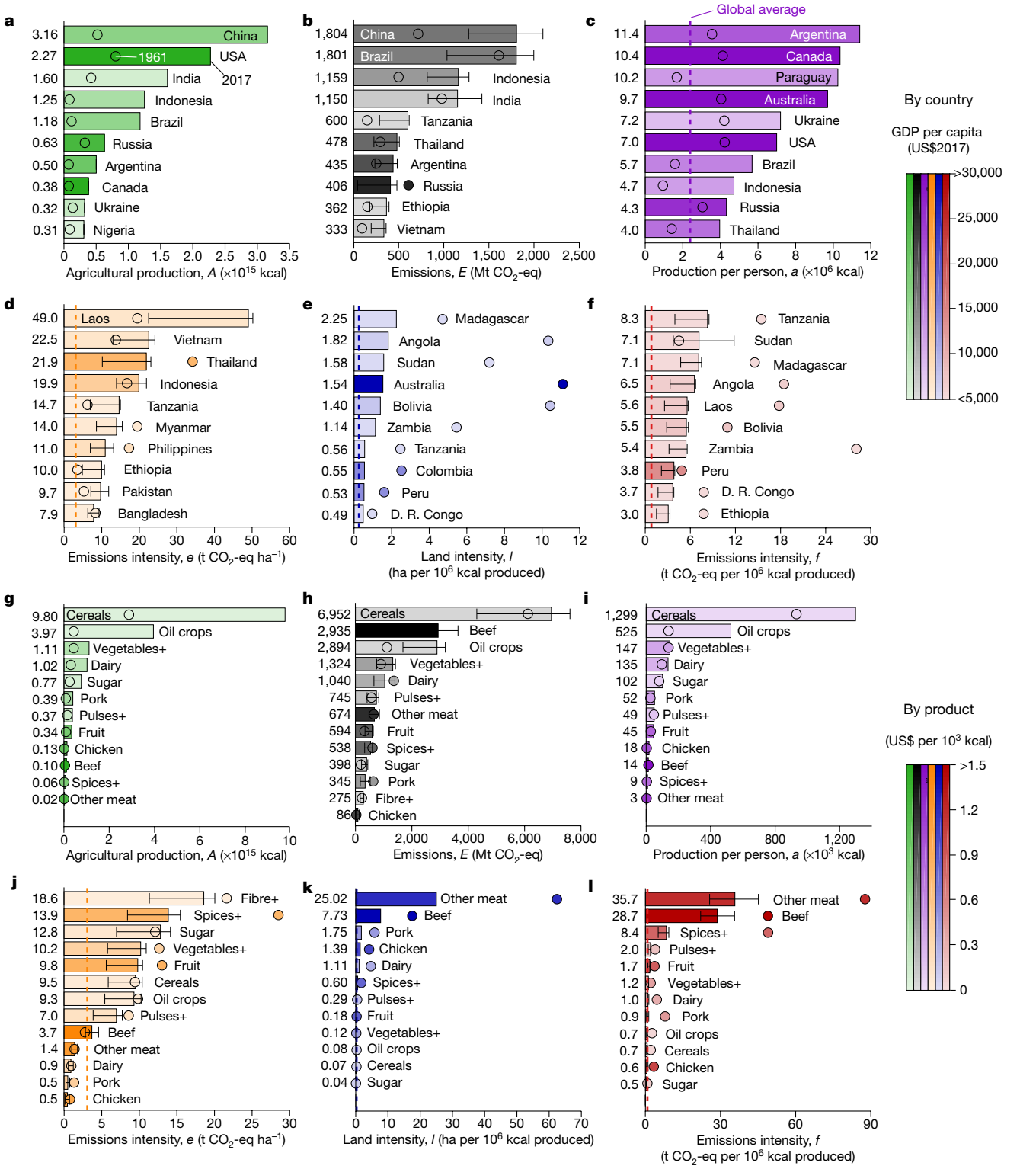

Fig. 4 | Intensities of the key *Pale* factors by country and by product. **a**–**f**, Highest 10 intensities for each of the *Pale* factors from the 30 highest-emitting countries in 2017 (bars coloured by GDP per capita). **g**–**l**, Intensities of major product groups in 2017 (bars coloured by value per production). Numbers are for 2017. The global averages in 2017 are shown by dashed lines. Dots are data for 1961. Error bars denote uncertainty ranges (68% intervals) for values in 2017, determined by uncertainties in land-use change emissions and in agricultural emissions, as well as uncertainties in the GWP_{100} values.

agricultural products (in units of calories produced, rather than mass), together producing 64% of global calories in 2017. There is substantial but imperfect overlap between these producers and the 10 largest emitters in Fig. 4b, which accounted for about 60% of all land-use emissions in 2017. Top emitters that are not also top producers tend to be less affluent countries with less access to farm inputs and greater reliance on bioenergy[32–34], such as Tanzania, Ethiopia and Vietnam (Fig. 4b). In turn, these countries often have particularly high land intensities of

agricultural production, as do poorer countries in which the quality of farmland tends to be low[32] (Fig. 4e). However, high emissions in affluent countries such as Australia and the USA are related to very high agricultural production per capita (Fig. 4c), with large shares of crops fed to livestock and food losses[35] and substantial international exports[36]. By contrast, the 10 countries with the greatest emissions intensity of land use include many tropical, carbon-dense countries in Southeast Asia in which rates of land-use change are especially high, such as Laos, Indonesia, Vietnam and Thailand (Fig. 4d). Thus, the countries with the highest emissions intensity of agricultural production include a mix of tropical and land-intensive systems that are uniformly poor and prone to agricultural expansion (Fig. 4f). The emissions intensity of production in these top 10 countries is 3–10 times the global average (Fig. 4f).

We also compare product groups in 2017 according to the *Pale* factors (Fig. 4g–l). Although cereals represent the largest source of both calories and emissions produced (Fig. 4g, h), the emissions per calorie of beef and other meat (buffalo, sheep and goats) are greater than the average intensity of other products by a factor of 30 (Fig. 4l). Although these red meats supply just 1% of total calories produced worldwide (Fig. 4g), they account for 25% (20–37%) of total land-use emissions (Fig. 4h; Table 1). Between 1961 and 2017, beef production increased much less (+144%) than chicken and pork production (483%; Fig. 4g), reflecting a widespread shift in the type of meat consumed, which reduced per capita meat emissions in 2017 by 44%. Incorporating other changes in the structure of calorie production in 1961–2017, per capita land-use emissions have decreased by 14%. Table 1 shows the share of land-use and global GHG emissions for each product group.

For the top 50 largest country–product sources of land-use emissions, Extended Data Fig. 10 shows changes in CO_2-equivalent emissions, per capita production, land intensity of production, and emissions intensity of land use over the most recent decade, 2006–2017. The list includes many large nations (for example, Indonesia, Brazil, China and USA) and major commodity crops and livestock (rice, maize, soybeans and cattle), as well as some less recognized sources (for example, Indonesian coconuts, Congolese cassava, Tanzanian maize and Sudanese sorghum). Although most sources show substantial decreases in their land intensity (that is, improving yields; Extended Data Fig. 10c), both per capita production and emissions intensity of land use often increase (Extended Data Fig. 10b, d). Efforts to substantially reduce global land-use emissions will probably need to address these specific sources.

Discussion and conclusions

Our results suggest that regions fall into three groups: (1) poorer regions where land-use change emissions are substantial and increasing (Latin America, sub-Saharan Africa and Southeast Asia); (2) emerging markets where land-use change emissions are small but agricultural emissions are increasing strongly (East Asia, South Asia and the Middle East); and (3) relatively affluent regions where land-use change emissions are often negative but agricultural emissions are substantial and flat (North America, Europe and Oceania).

The drivers and sources of emissions in each group point to both mitigation opportunities and emissions that may be especially difficult to avoid. For countries in the first category, the largest mitigation opportunities almost certainly lie in limiting land-use change[37], especially conversions of carbon-dense tropical forests to soybeans, rice, maize and oil palm. For countries in both the second and third categories, decreases in the emissions intensity of agricultural production are critical, and may be achieved by improved input efficiencies[38,39], better soil and livestock waste management[40,41], reductions in food waste[42,43] or behavioural and policy-driven changes in agricultural demand[44,45]. Future work may evaluate how specific shifts in diets and the extent and intensity of agricultural production (for example, via international trade) could minimize the emissions intensity of land use, as well as how climate adaptation efforts (for example, through increased resilience of agricultural systems and supply chains) could affect agricultural production and emissions.

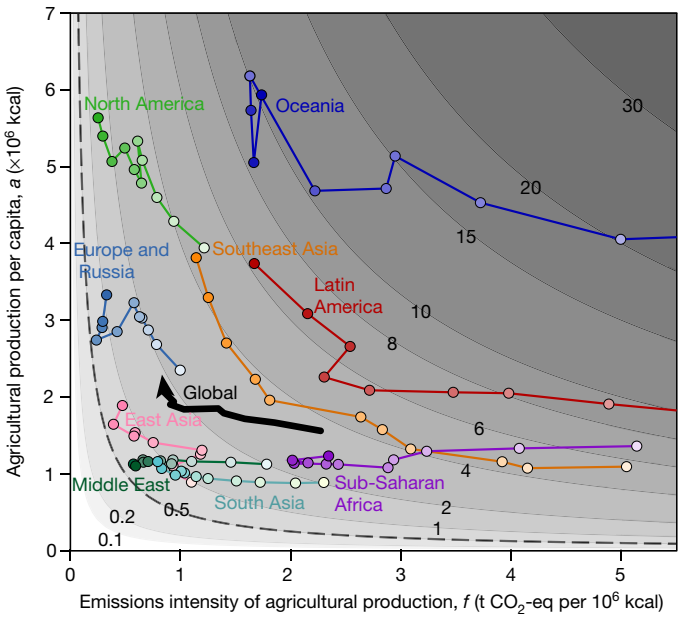

Fig. 5 | Trends in per capita land-use emissions. Coloured lines show regional trends in agricultural production per capita (*a*) and the corresponding emissions intensity of that production (*f*) from 1961 to 2017 (light to dark points). The bold black line shows the corresponding global trend. Background contours are in units of tons of CO_2-equivalent emissions per capita. Even in the most affluent regions, where land-use change emissions are small, per capita emissions have not decreased below 0.5 t CO_2-eq per person (dashed black contour line).

However, aggregate land-use emissions are not convincingly decreasing in any region (Fig. 2). Global population continues to rise, and per capita emissions are nowhere less than 0.5 t CO_2-eq yr^{-1}—and substantially higher in most nations (Fig. 5). Therefore, although our results help to target high-priority countries, processes and products for mitigation, they also suggest the difficulty of drastically reducing land-use emissions without comparably drastic changes in agricultural production and/or agricultural practices (Fig. 5, Extended Data Fig. 11). However, recent research has demonstrated some promising mitigation options: rice cultivars and non-continuous rice-paddy flooding practices may achieve substantial reductions in CH_4 while also increasing yields[46,47], and dietary supplements for cattle reduced methane emissions up to 95% in pilot studies[48]. Non-technical factors such as political inertia, weak governance and lack of finance may therefore be key barriers[49].

Rising global population and agricultural production per capita have increased land-use emissions for more than half a century. Future growth in population and incomes is likely to boost food demand further and hinder efforts to reduce land-use emissions. Moreover, despite recognition that current climate targets may depend upon large reductions in agricultural emissions[23,50], the related technological and policy challenges may rival those of net-zero emissions energy systems; agriculture may always entail substantial GHG emissions. For example, even if global average land-use emissions per capita reach the current level in Europe (that is, 0.5–1 t CO_2-eq per person per year; light blue curve in Fig. 5), global emissions would be 4.7–12.7 Gt CO_2-eq yr^{-1} in 2100 under United Nations' population projections—a quantity that may be difficult to reconcile with ambitious international climate goals. Thus, even in regions where per capita land-use emissions are now lowest, substantial changes in the demand for and production of food are still

needed; current climate goals require that land-use policies, practices and efficiencies improve everywhere.

Online content

Any methods, additional references, Nature Research reporting summaries, source data, extended data, supplementary information, acknowledgements, peer review information; details of author contributions and competing interests; and statements of data and code availability are available at https://doi.org/10.1038/s41586-020-03138-y.

1. Foley, J. A. et al. Global consequences of land use. *Science* **309**, 570–574 (2005).
2. Haddad, N. M. et al. Habitat fragmentation and its lasting impact on Earth's ecosystems. *Sci. Adv*. **1**, e1500052 (2015).
3. Marques, A. et al. Increasing impacts of land use on biodiversity and carbon sequestration driven by population and economic growth. *Nat. Ecol. Evol*. **3**, 628–637 (2019).
4. Newbold, T. et al. Global effects of land use on local terrestrial biodiversity. *Nature* **520**, 45–50 (2015).
5. Houghton, R. A. Land-use change and the carbon cycle. *Glob. Change Biol*. **1**, 275–287 (1995).
6. Gruber, N. & Galloway, J. An Earth-system perspective of the global nitrogen cycle. *Nature* **451**, 293–296 (2008).
7. Houghton, R. A. et al. Carbon emissions from land use and land-cover change. *Biogeosciences* **9**, 5125–5142 (2012).
8. Carlson, K. M. et al. Greenhouse gas emissions intensity of global croplands. *Nat. Clim. Chang*. **7**, 63–68 (2017).
9. Matthews, H. D. & Caldeira, K. Stabilizing climate requires near-zero emissions. *Geophys. Res. Lett*. **35**, L04705 (2008).
10. Smith, S. M. et al. Equivalence of greenhouse-gas emissions for peak temperature limits. *Nat. Clim. Chang*. **2**, 535–538 (2012).
11. Rogelj, J., Meinshausen, M., Schaeffer, M., Knutti, R. & Riahi, K. Impact of short-lived non-CO2 mitigation on carbon budgets for stabilizing global warming. *Environ. Res. Lett*. **10**, 075001 (2015).
12. Collins, W. J. et al. Increased importance of methane reduction for a 1.5 degree target. *Environ. Res. Lett*. **13**, 054003 (2018).
13. Peters, G. P. et al. Key indicators to track current progress and future ambition of the Paris Agreement. *Nat. Clim. Chang*. **7**, 118–122 (2017).
14. Le Quéré, C. et al. Drivers of declining CO_2 emissions in 18 developed economies. *Nat. Clim. Chang*. **9**, 213–217 (2019).
15. FAO. *FAOSTAT* http://faostat.fao.org/ (Food and Agriculture Organization of the United Nations, 2019).
16. Houghton, R. A. The annual net flux of carbon to the atmosphere from changes in land use, 1850–1990. *Tellus B* **51**, 298–313 (1999).
17. Carlson, K. M. et al. Carbon emissions from forest conversion by Kalimantan oil palm plantations. *Nat. Clim. Chang*. **3**, 283–287 (2013).
18. Morton, D. C. et al. Cropland expansion changes deforestation dynamics in the southern Brazilian Amazon. *Proc. Natl Acad. Sci. USA* **103**, 14637–14641 (2006).
19. Barona, E., Ramankutty, N., Hyman, G. & Coomes, O. T. The role of pasture and soybean in deforestation of the Brazilian Amazon. *Environ. Res. Lett*. **5**, 024002 (2010).
20. Yan, X., Akiyama, H., Yagi, K. & Akimoto, H. Global estimations of the inventory and mitigation potential of methane emissions from rice cultivation conducted using the 2006 Intergovernmental Panel on Climate Change Guidelines. *Glob. Biogeochem. Cycles* **23**, GB2002 (2009).
21. Huber, V., Neher, I., Bodirsky, B. L., Hofner, K. & Schellnhuber, H. J. Will the world run out of land? A Kaya-type decomposition to study past trends of cropland expansion. *Environ. Res. Lett*. **9**, 024011 (2014).
22. Hosonuma, N. et al. An assessment of deforestation and forest degradation drivers in developing countries. *Environ. Res. Lett*. **7**, 044009 (2012).
23. IPCC. *Climate Change and Land* (eds Shukla, P. R. et al.) (IPCC, 2019); https://www.ipcc.ch/srccl/
24. Hansis, E., Davis, S. J. & Pongratz, J. Relevance of methodological choices for accounting of land use change carbon fluxes. *Glob. Biogeochem. Cycles* **29**, 1230–1246 (2015).
25. Davis, S. J., Burney, J. A., Pongratz, J. & Caldeira, K. Methods for attributing land-use emissions to products. *Carbon Manag*. **5**, 233–245 (2014).
26. Griscom, B. W. et al. Natural climate solutions. *Proc. Natl Acad. Sci. USA* **114**, 11645–11650 (2017).
27. US EPA. *Global Anthropogenic Non-CO_2 Greenhouse Gas Emissions: 1990–2030*. Report No. 430-R-12-006 (US Environmental Protection Agency, 2012); www.epa.gov/sites/production/files/2016-08/documents/epa_global_nonco2_projections_dec2012.pdf
28. Janssens-Maenhout, G. et al. EDGAR v4.3.2 Global Atlas of the three major greenhouse gas emissions for the period 1970–2012. *Earth Syst. Sci. Data* **11**, 959–1002 (2019).
29. Houghton, R. A. & Nassikas, A. A. Global and regional fluxes of carbon from land use and land cover change 1850–2015. *Glob. Biogeochem. Cycles* **31**, 456–472 (2017).
30. Friedlingstein, P. et al. Global carbon budget 2019. *Earth Syst. Sci. Data* **11**, 1783–1838 (2019).
31. Gibbs, H. K. et al. Tropical forests were the primary sources of new agricultural land in the 1980s and 1990s. *Proc. Natl Acad. Sci. USA* **107**, 16732–16737 (2010).
32. Sánchez, P. A. Tripling crop yields in tropical Africa. *Nat. Geosci*. **3**, 299–300 (2010).
33. Felix, M. & Gheewala, S. H. A review of biomass energy dependency in Tanzania. *Enrgy. Proced*. **9**, 338–343 (2011).
34. Sola, P., Ochieng, C., Yila, J. & Iiyama, M. Links between energy access and food security in sub Saharan Africa: an exploratory review. *Food Secur*. **8**, 635–642 (2016).
35. Gustavsson, J., Cederberg, C. & Sonesson, U. *Global Food Losses and Food Waste: Extent, Causes and Prevention* (Food and Agriculture Organization of the United Nations, 2011); http://www.fao.org/3/a-i2697e.pdf
36. D'Odorico, P., Carr, J. A., Laio, F., Ridolfi, L. & Vandoni, S. Feeding humanity through global food trade. *Earths Futur*. **2**, 458–469 (2014).
37. Lamb, A. et al. The potential for land sparing to offset greenhouse gas emissions from agriculture. *Nat. Clim. Chang*. **6**, 488–492 (2016).
38. Clark, M. & Tilman, D. Comparative analysis of environmental impacts of agricultural production systems, agricultural input efficiency, and food choice. *Environ. Res. Lett*. **12**, 064016 (2017).
39. Kanter, D. R. & Searchinger, T. D. A technology-forcing approach to reduce nitrogen pollution. *Nat. Sustain*. **1**, 544–552 (2018); author correction **1**, 719 (2018).
40. Paustian, K. et al. Climate-smart soils. *Nature* **532**, 49–57 (2016).
41. Herrero, M. et al. Greenhouse gas mitigation potentials in the livestock sector. *Nat. Clim. Chang*. **6**, 452–461 (2016).
42. Ritchie, H., Reay, D. S. & Higgins, P. Beyond calories: a holistic assessment of the global food system. *Front. Sustain. Food Syst*. **2**, 57 (2018).
43. Bajželj, B. et al. Importance of food-demand management for climate mitigation. *Nat. Clim. Chang*. **4**, 924–929 (2014).
44. Poore, J. & Nemecek, T. Reducing food's environmental impacts through producers and consumers. *Science* **360**, 987–992 (2018); erratum **363**, eaaw9908 (2019).
45. Stehfest, E. Food choices for health and planet. *Nature* **515**, 501–502 (2014).
46. Jiang, Y. et al. Water management to mitigate the global warming potential of rice systems: a global meta-analysis. *Field Crops Res*. **234**, 47–54 (2019).
47. Jiang, Y. et al. Higher yields and lower methane emissions with new rice cultivars. *Glob. Change Biol*. **23**, 4728–4738 (2017).
48. Roque, B. M. et al. Effect of the macroalgae *Asparagopsis taxiformis* on methane production and rumen microbiome assemblage. *Animal Microbiome* **1**, 3 (2019); correction **1**, 4 (2019).
49. Lamb, W. F. & Minx, J. C. The political economy of national climate policy: architectures of constraint and a typology of countries. *Energy Res. Soc. Sci*. **64**, 101429 (2020).
50. Clark, M. A. et al. Global food system emissions could preclude achieving the 1.5° and 2° C climate change targets. *Science* **370**, 705–708 (2020).

Methods

Land-use emissions

The major processes of land-use emissions are: (1) CO_2 emissions from transitions in land use (which could include, for example, the clearing of native habitat for agriculture or changes in agricultural use), harvesting of forest products, peat drainage and peat burning; (2) uptake of CO_2 from regrowth of forests and recovery of abandoned agricultural land (that is, negative emissions); (3) N_2O released from soils related to the application of nitrogenous fertilizer, manure applied to soils, manure left on pasture, and agricultural residues left on pasture; (4) CH_4 from enteric fermentation of livestock; (5) CH_4 and N_2O from manure management; (6) CH_4 from rice cultivation; and (7) CH_4 and N_2O from burning of agricultural residues. Sinks and sources of (1) and (2) together represent emissions from land-use change (sometimes also referred to as 'forestry and other land use' emissions). The other sources, (3)–(7), represent emissions from agricultural activities.

In keeping with reporting requirements of the United Nations Framework Convention on Climate Change for fossil fuel emissions, we assign these land-use emissions to the country in which they are physically produced (that is, production-based accounting; as opposed to where related goods are ultimately consumed).

Estimates of land-use change emissions

To estimate emissions caused by different land-use change, including conversion of natural land to cropland ('LUC-Crops' in Fig. 1) or pasture ('LUC-Pasture'), as well as harvest of forest products ('Wood harvest') and recovery and abandonment of cropland or pasture ('Agricultural abandonment'), we developed the carbon-bookkeeping model BLUE (bookkeeping of land-use emissions; the model and the attribution methods to different activities are described in ref. [24]). The BLUE model offers the unique option to track the contribution of each past year's land-use activities to the current year's emissions. Such a feature allows emissions to be attributed to specific products (see section 'Distribution of land-use change emissions to products' for details).

The BLUE model uses gridded estimates at 0.25° resolution of current and historical land-use activities produced by the harmonized land-use change dataset LUH2[51] (http://luh.umd.edu), as updated for the global annual carbon budget 2019[30], together with a global potential vegetation map[52] and biome-specific carbon values and response functions[16,53]. Land-use activities include expansion and abandonment of cropland, pasture and rangelands, as well as wood harvesting. Sub-grid scale transitions—for example, due to shifting cultivation—are captured. The shifting cultivation is based on a new dataset that uses high-resolution remote sensing to map the current extent of shifting cultivation and uses large surveys to estimate long-term trends[54]. Similar to other bookkeeping models, BLUE assumes that abandoned land returns to its potential vegetation type but accounts for permanent degradation by assigning lower carbon densities to secondary than to primary (never converted) land. The treatment of rangelands is conditional on the potential vegetation type: conversions from/to rangelands affecting potentially forested land are treated as conversions from/to pasture, whereas conversions affecting grasslands lead only to degradation of primary to secondary lands. Using BLUE, we generated spatially explicit and use-specific estimates of carbon emissions from changes in land use during each year between 850 and 2017.

To calculate emissions from the extraction of biomass from forest and other natural vegetation types (which may or may not entail conversion of unmanaged land to cropland or pasture; see ref. [51]), we used gridded, historical estimates of the area harvested as provided as part of LUH2. Carbon fluxes to and from soils were calculated using the BLUE model, as was the uptake of carbon by recovering vegetation.

Emissions from peat drainage and peat burning are not captured by the BLUE model directly and are added from external datasets: for peat drainage, we use the new country-level estimates by the Food and Agriculture Organization (FAO) for emissions associated with drainage of organic soils for cultivation and grazed grasslands since 1990[15]. For 1961–1990 we keep the drainage emissions constant at the 1990 value[55] for boreal and temperate peatlands; for tropical peatlands in equatorial Asia, the drainage emissions are interpolated from 0 in 1980 to the 1990 value[56]. For carbon emissions associated with peat burning, we use the Global Fire Emission Database[57].

Net land-use change emissions estimated by our BLUE model are within the range of previously published estimates[24], and have been adopted by the Global Carbon Project as one of two bookkeeping models providing estimates for the global net land-use change flux[30]. Importantly, BLUE offers the unique option to attribute the estimated emissions to the year in which the land-use change happened ('temporal accounting'; ref. [24]). This is in contrast to other models that aggregate emissions on the basis of when they occur, that is, which aggregate effects of land-use changes that happened in different years. Preserving the disaggregated results in this way allows us to integrate the emissions associated with land-use changes in a given year and redistribute those emissions differently over time (see section 'Distribution of land-use change emissions over time'). This may be advantageous in crafting land-use policies (see, for example, ref. [25]). Finally, we aggregate our spatially explicit estimates of net carbon (CO_2) emissions from land-use changes into each of the countries for which the FAO provides agricultural data.

Estimates of agricultural emissions

GHG emissions from agriculture in each of 229 countries/areas (collectively referred to as 'countries' in this study) in 1961–2017, including CH_4 emissions from enteric fermentation of livestock and rice cultivation, N_2O emissions from synthetic fertilizers, manure applied to soils, manure left on pasture, agricultural residues left on pasture, and CH_4 and N_2O emissions from manure management and burning of agricultural residues, were obtained from the FAO[15] (data are available at http://faostat.fao.org/). The FAO developed a global database of GHG emissions from agriculture with country- and product-level detail, using activity data from the FAOSTAT database and Intergovernmental Panel on Climate Change (IPCC) Tier 1 methodology. More details can be found in Tubiello et al.[58] and the FAOSTAT database (http://faostat.fao.org/). For the few government systems that have changed between 1961 and 2017, we allocated the data of the original countries to their successor countries based on the ratios in recent years.

Emissions from rice cultivation and synthetic fertilizers were computed at Tier 1 level, using national-level FAOSTAT statistics of harvested rice area and fertilizer consumption, respectively. Emissions from enteric fermentation, manure management, manure applied to soils, and manure left on pasture were computed at Tier 1 level, using FAOSTAT statistics of animal numbers. Emissions from agricultural residues left on pasture and burning of agricultural residues were computed at Tier 1 level, using national-level FAOSTAT statistics of crop yield and harvested area. To calculate emissions from rice cultivation, a regional-level distribution of rice management types was used. For synthetic fertilizers and manure management, indirect emissions due to volatilization and leaching were also included. A time series of crop-specific fertilizer consumption data was used in this study, with crop-specific fertilizer application rates developed by Conant et al.[59] (1961–2008; the application rates in 2008 were used for years after 2008) along with harvested areas obtained from the FAO, and the national totals were then scaled to the FAOSTAT statistics. In order to calculate mature N_2O emissions, an intermediate dataset was generated, which contained animal- and region-specific values, including manure N excretion rates, manure fractions disposed to different manure management systems and left on pasture, manure application rates to cropland, and manure management system losses[58]. Because CH_4 emissions from manure management are sensitive to the type of management and temperature, region- and temperature-specific IPCC

emissions factors[60] were used. To calculate mature CH_4 emissions, average annual temperatures by country obtained from the FAO global agro-ecological zone database[61] were used, which was in an exception to the general Tier 1 approach, given that IPCC guidelines provide no such data as default.

Although there are many examples of fossil fuels being burned in support of land-use activities (for example, to produce agricultural inputs, build and operate agricultural machinery, and transport agricultural and forest products), we do not consider the CO_2 emissions related to such fossil fuel combustion in this study. Such fossil fuel emissions related to agricultural sectors have been quantified and analysed in detail by previous studies[62–64].

Drivers (activity data)

We used population data for the years 1961 through 2017 (and also 2100) from the United Nations Population Division's 2019 Revision of the World Population Prospects[15,65] (data are available at http://faostat.fao.org/).

Production data of crops, animal products and roundwood for each country for 1961–2017 were obtained from the FAO[15] (data are available at http://faostat.fao.org/). We obtained FAO data on each country's production of 150 distinct food crops (including cereals, fruits and vegetables, pulses, oil and sugar crops, and spices) and 7 meat and dairy products (including pork, beef meat, buffalo meat, sheep and goat meat, poultry meat, eggs and milk) by mass. Where we discuss production of food crops, and meat and dairy products in particular, we have converted production data from units of mass (metric tonnes) into units of energy content (kilocalories)[8,42] using published conversion factors[66] (data available at http://www.fao.org/docrep/003/X9892E/X9892e05.htm#P8217_125315). We obtained FAO data on each country's production of 11 different fibre crops by mass (metric tonnes) and production of roundwood by volume (cubic metres).

Land-use area data of 150 food crops and 11 fibre crops harvested for each country in 1961–2017 were obtained from the FAO[15]. Data on the area of pasture in each country were taken from the FAO[15]. We also calculated the area occupied by different livestock types using gridded livestock density[67,68] (0.05° in 2005; data are available at http://www.fao.org/livestock-systems/en/) together with FAO data on the number of 7 livestock types in each country in 1961–2017[15], and assuming that livestock densities in each country remained constant at 2005 levels during the period 1961–2017. The total livestock areas calculated in this way were then adjusted to match national pasture areas from the FAO, and were then used to calculate land-use intensity and emissions intensity of each livestock type.

Distribution of land-use change emissions over time

After conversion of land from a natural to a managed system, the oxidation of carbon present in biomass, soils and products releases the GHG CO_2 to the atmosphere. In contrast to emissions from burning of fossil fuels, the release of these gases occurs over time, often many years. In BLUE, these legacy emissions depend on the type and extent of land-use transition and the shape of the (observation-based) response curves that describe the adjustment of biomass, fast and slow soil carbon pools to the new values of the managed system. The biomass attributed to the three product pools decays with a lifetime of 1, 10 and 100 years, respectively. Similarly to the legacy emissions from decay of biomass and soil carbon, carbon uptake due to regrowth also occurs slowly over time, described by response curves of how quickly biomass and soil carbon recover upon abandonment of agricultural land or after a harvest event. All response curves are specific for the different types of natural ecosystem and the different types of managed system.

Our base results reflect CO_2 emissions occurring in each year due to past changes in land use ('legacy' emissions), but split the emissions occurring in a given year to the various land-use change events in the past that caused the emissions. Different methodological assumptions have also been evaluated, for example, all future emissions from a change in land use assigned to the year of the change ('committed' emissions) and committed emissions amortized uniformly over 20 years ('uniformly distributed' emissions) (Extended Data Fig. 1).

Distribution of land-use change emissions to products

There are several methods for allocating land-use change emissions to specific agricultural products. We distributed emissions from conversion to cropland (LUC-Crops) and pasture (LUC-Pasture) among different types of crops and livestock, respectively. We distributed emissions from a region in a year according to annual national statistics of land areas (or production) of different agricultural products obtained from the FAO. Our base results reflect land-use change emissions allocating among crops and livestock by land area used (cropland area and livestock area, respectively). This method of allocation assumes that land-use emissions are closely related to land area, which is a direct and indivisible characteristic of land use. Different methodological assumptions have also been evaluated, for example, allocating among crops and livestock by change in land area, calories of production, mass of production and change in mass of production (Extended Data Fig. 1). Detailed discussion about these different attribution methods can be found in Davis et al.[25]. We allocated emissions from harvest of forest products (wood harvest) to wood products. Carbon uptake from agriculture abandonment is not included in the product allocation.

Allocation of emissions related to feed crops

Our base case allocates the emissions related to livestock feed to the crops themselves. We also evaluate another accounting: allocating the feed crop emissions to the livestock that consumed the feed. Feed quantities of each crop in each country in 1961–2017 were obtained from the FAO Food Balance Sheet[15], and were then used to calculate the fractions of crop production used as livestock feed to shift emissions related to feed crops from crop production to livestock production. We distributed those emissions among different types of livestock based on estimates of the relative livestock energy requirements of each type, which were calculated using FAOSTAT statistics of animal numbers[15] and energy requirement per animal obtained from Herrero et al.[69]. The results of the two accountings of the feed crops emissions are shown in Extended Data Fig. 2.

Emission metrics

All aggregate GHG emissions are converted into CO_2-equivalents (CO_2-eq) using GWPs with a 100-year time horizon (GWP_{100}), which is also used within the United Nations Framework Convention on Climate Change and the IPCC report[70]. The GWP_{100} values are obtained from the IPCC Fifth Assessment Report (AR5)[71]. The GWP_{100} value for CH_4 in the IPCC AR5 (34) is higher than that in previous IPCC assessments (21–25), whereas the GWP_{100} value for N_2O in the IPCC AR5 (298) is similar to that in previous IPCC assessments (296–310). As suggested by AR5[71], we evaluate the uncertainty related to GWP_{100} by assuming an uncertainty of ±40% for CH_4 and ±30% for N_2O. The emission estimates with the GWP_{100} uncertainty ranges are shown in Extended Data Fig. 3.

In addition, to assess the sensitivity of the results to metric choices, we estimate emissions using GWP*[72,73]. Details of the GWP* calculation can be found in Allen et al.[72] and Cain et al.[73]. In the GWP* calculation, a step change in emission rate of a short-lived climate pollutant (SLCP; ΔE_{SLCP} tonnes per year) is equivalent to a one-off pulse emission of $\Delta E_{SLCP} \times GWP_H \times H$ tonnes of CO_2 (denoted CO_2-e*), where GWP_H is the conventional GWP relative to CO_2 integrated over a time horizon of H years. Here, as suggested by Allen et al.[72], we used $H = 100$, and considered change in the SLCP emission rate over the preceding 20 years to reduce the volatility of GWP* emissions. For CO_2 and N_2O, CO_2-eq and CO_2-e* emissions are identical. For CH_4, annual CO_2-e* emissions track the rate of change of emissions, unlike CO_2-eq, which tracks the emissions themselves. Long-term trends in total land-use emissions

calculated with GWP* are generally consistent with the results calculated with GWP_{100} (Extended Data Fig. 3). CO_2-e* emissions are sometimes negative in Europe and Russia, reflecting the decreasing CH_4 emissions in the region.

Pale identity

We discuss our analysis of land-use emissions as factors of a *Pale* identity (equation (1)), as described in the main text. To facilitate discussion of important regional differences and trends, these terms were disaggregated into nine regions (Fig. 1e), denoted by subscript r, the sum of which equals the world total:

$$E = \sum_r E_r = \sum_r P_r a_r l_r e_r \,. \tag{2}$$

Similarly, to facilitate discussion of important differences across sources and products, we also disaggregate the *Pale* analysis into major sources and groups of products, s:

$$E = \sum_s E_s = \sum_s P\left(\frac{A_s}{P}\right)\left(\frac{L_s}{A_s}\right)\left(\frac{E_s}{L_s}\right) = \sum_s P a_s l_s e_s. \tag{3}$$

Thus, we have disaggregated the emission variable (E) into two sectors (land-use change and agricultural activities), with other variables (A, L) aggregated into totals. We have also disaggregated each of these variables (A, E, L) into 14 groups of products: 7 food crops, 5 types of meat and dairy product, fibre crops and wood products (see Extended Data Table 2 for a more detailed listing of products and their categorization). Once disaggregated, agricultural production can be converted from units of mass into more accessible units[8,42]. When focusing on the food value of crops, meat and dairy products, we convert units of mass into calories using crop- and product-specific conversion factors[66] and exclude production data of fibre and wood.

Uncertainty assessment

We conducted comprehensive uncertainty analyses to provide uncertainty ranges around our central estimates. For our estimates of land-use change emissions, we conducted five sensitivity simulations to assess uncertainties in major model assumptions underlying the BLUE estimates. Three simulations were performed to assess the uncertainty associated with biogeochemical parameters, using biome-specific carbon values derived from dynamic global vegetation models used in the Global Carbon Budget (GCB) study that provided output per plant functional type (JSBACH, ISAM and ORCHIDEE-CNP)[74]. Two additional simulations were performed to assess the uncertainty associated with the land-use change data (LUH2), using the low and high historical reconstructions that have recently been produced for CMIP6[75].

For our estimates of agriculture emissions, we followed the IPCC 2006 guidelines[60] and adopted a Monte Carlo approach to assess the uncertainty range of emissions by varying activity data, parameter values and emission factors and running 1,000 simulations. Similar to the uncertainty analysis performed by Tubiello et al.[58], we applied IPCC default uncertainty ranges for activity data, parameters and emission factors for each agricultural process, as prescribed by the IPCC guidelines[60] (see Supplementary Table 1).

Following the most recent GCB study[30], we report uncertainties as a 68% probability range around our central estimates, which reflects the difficulty of characterizing the uncertainty in the land-use emissions (particularly the land-use change emissions) and provides an indication of our current capability. The full range of the six BLUE simulations (five sensitivity tests and our base case), which is close to the 68% uncertainty range reported by the GCB study, is assumed to be the 68% uncertainty range of our estimates of land-use change emissions. To obtain the uncertainty range of total land-use emissions, the six BLUE simulations of land-use change emissions were then combined with the Monte Carlo simulations of agriculture emissions (uncertainties in GWP_{100} values are also included) to generate six Monte Carlo ensembles (6,000 total estimates). The 68% interval for each Monte Carlo ensemble was collected, and the maximum range of the six intervals collected was reported as the overall 68% uncertainty range (compared to directly reporting 68% interval across all 6,000 estimates, this approach often provides a greater uncertainty range). The base case is reported as our central estimates.

We also compare our estimates of land-use emissions with other existing inventories. Our estimates of agriculture emissions are generally consistent with the EDGARv5.0[28] and the US EPA[27] emission inventories in all the regions (Extended Data Fig. 4), suggesting a relatively high confidence level. Our base case estimates of land-use change emission trends during the whole period (legacy emissions) are also quite consistent with the estimates of Houghton and Nassikas[29] (H&N; the other bookkeeping model used in the GCB study) in many regions (Extended Data Figs. 5, 6). We also performed an additional *Pale* analysis by using agricultural emissions from the FAO combined with the average of land-use change emissions from two bookkeeping models (BLUE and H&N, which is the central estimate in the GCB study). Our estimates of trends in land-use emissions and *Pale* factors are also generally consistent with the results that used the average of two bookkeeping models (Extended Data Figs. 6, 7). However, trends in land-use change emissions in North America and East Asia are more different in the two bookkeeping models, suggesting a relatively lower confidence level in the two regions (Extended Data Fig. 5).

Data availability

The agricultural emissions data are curated by the FAO and freely available from FAOSTAT at http://faostat.fao.org/. Land-use change emissions (BLUE) data and all of our results are available at https://sustsys.ess.uci.edu/CALUE.html and https://doi.org/10.6084/m9.figshare.12248735.

Code availability

Computer codes or algorithms used to generate results that are reported in the paper and central to the main claims are available at https://github.com/ChaopengHong/Land-use_Emissions.

51. Hurtt, G. C. et al. Harmonization of global land use change and management for the period 850–2100 (LUH2) for CMIP6. *Geosci. Model Dev.* **13**, 5425–5464 (2020).
52. Pongratz, J., Reick, C., Raddatz, T. & Claussen, M. A reconstruction of global agricultural areas and land cover for the last millennium. *Glob. Biogeochem. Cycles* **22**, GB3018 (2008).
53. Houghton, R. A. et al. Changes in the carbon content of terrestrial biota and soils between 1860 and 1980: a net release of CO_2 to the atmosphere. *Ecol. Monogr.* **53**, 235–262 (1983).
54. Heinimann, A. et al. A global view of shifting cultivation: recent, current, and future extent. *PLoS One* **12**, e0184479 (2017).
55. Leifeld, J., Wust-Galley, C. & Page, S. Intact and managed peatland soils as a source and sink of GHGs from 1850 to 2100. *Nat. Clim. Chang.* **9**, 945–947 (2019).
56. Hooijer, A. et al. Current and future CO_2 emissions from drained peatlands in Southeast Asia. *Biogeosciences* **7**, 1505–1514 (2010).
57. van der Werf, G. R. et al. Global fire emissions estimates during 1997–2016. *Earth Syst. Sci. Data* **9**, 697–720 (2017).
58. Tubiello, F. N. et al. The FAOSTAT database of greenhouse gas emissions from agriculture. *Environ. Res. Lett.* **8**, 015009 (2013).
59. Conant, R. T., Berdanier, A. B. & Grace, P. R. Patterns and trends in nitrogen use and nitrogen recovery efficiency in world agriculture. *Glob. Biogeochem. Cycles* **27**, 558–566 (2013).
60. IPCC. *Guidelines for National Greenhouse Gas Inventories* Vol. 4 (IPCC, 2006).
61. FAO. *Global Agro-Ecological Zones (GAEZ v3.0)* http://www.fao.org/nr/gaez/en/ (Food and Agriculture Organization of the United Nations, 2012).
62. Davis, S. J., Peters, G. P. & Caldeira, K. The supply chain of CO_2 emissions. *Proc. Natl Acad. Sci. USA* **108**, 18554–18559 (2011).
63. Davis, S. J. & Caldeira, K. Consumption-based accounting of CO_2 emissions. *Proc. Natl Acad. Sci. USA* **107**, 5687–5692 (2010).
64. Peters, G. P. & Hertwich, E. G. CO_2 embodied in international trade with implications for global climate policy. *Environ. Sci. Technol.* **42**, 1401–1407 (2008).
65. UN. *World Population Prospects 2019: Highlights*. Report No. ST/ESA/SER.A/423 (United Nations, 2019); https://population.un.org/wpp/Publications/Files/WPP2019_Highlights.pdf

66. FAO. *Food Balance Sheets: A Handbook* (Food and Agriculture Organization of the United Nations, 2001); http://www.fao.org/docrep/pdf/011/x9892e/x9892e00.pdf
67. Robinson, T. P., Franceschini, G. & Wint, W. The Food and Agriculture Organization's gridded livestock of the world. *Vet. Ital.* **43**, 745–751 (2007).
68. Robinson, T. P. et al. Mapping the global distribution of livestock. *PLoS One* **9**, e96084 (2014).
69. Herrero, M. et al. Biomass use, production, feed efficiencies, and greenhouse gas emissions from global livestock systems. *Proc. Natl Acad. Sci. USA* **110**, 20888–20893 (2013).
70. IPCC. *Climate Change 2014: Mitigation of Climate Change* (eds Edenhofer, O. et al.) (Cambridge Univ. Press, 2014).
71. IPCC. *Climate Change 2013: The Physical Science Basis* (eds Stocker, T. F. et al.) (Cambridge Univ. Press, 2013).
72. Allen, M. R. et al. A solution to the misrepresentations of CO_2-equivalent emissions of short-lived climate pollutants under ambitious mitigation. *npj Clim. Atmos. Sci* **1**, 16 (2018).
73. Cain, M. et al. Improved calculation of warming-equivalent emissions for short-lived climate pollutants. *npj Clim. Atmos. Sci*. **2**, 29 (2019).
74. Le Quéré, C. et al. Global carbon budget 2018. *Earth Syst. Sci. Data* **10**, 2141–2194 (2018).
75. Lawrence, D. M. et al. The Land Use Model Intercomparison Project (LUMIP) contribution to CMIP6: rationale and experimental design. *Geosci. Model Dev*. **9**, 2973–2998 (2016).

Acknowledgements A. LoPresti helped with preliminary analysis; E. Hansis made important contributions to the development of the BLUE model. K. Hartung helped with additional BLUE simulations. We thank A. Jain and D. Goll for providing ISAM and ORCHIDEE-CNP data. We thank R. A. Houghton and A. A. Nassikas for providing data from ref. [29]. We thank R. T. Conant for providing crop-specific fertilizer application rates. The manuscript also benefitted from discussions with R. Andrew, L. Chini, H. van Grinsven, K. Hartung, R. A. Houghton, S. Kloster, E. Lambin, D. Lobell, P. Meyfroidt, G. Peters, Y. Qin, T. Raddatz, J. Randerson, M. Raupach, D. Tong and T. West. C.H., J.A.B. and S.J.D. were supported by the US National Science Foundation and US Department of Agriculture (INFEWS grant EAR 1639318). J.P. and J.E.M.S.N. were supported by the German Research Foundation's Emmy Noether Programme (PO1751/1-1). R.B.J. acknowledges support from the Gordon and Betty Moore Foundation (grant GBMF5439).

Author contributions S.J.D., C.H., J.A.B. and J.P. conceived the study. C.H., S.J.D. and J.A.B. performed the analyses, with support from J.P. and J.E.M.S.N. on datasets, and from N.D.M and R.B.J. on analytical approaches. C.H. and S.J.D. led the writing with input from all co-authors. All co-authors reviewed and commented on the manuscript.

Competing interests The authors declare no competing interests.

Additional information

Supplementary information The online version contains supplementary material available at https://doi.org/10.1038/s41586-020-03138-y.

Correspondence and requests for materials should be addressed to C.H., J.A.B. or S.J.D.

Peer review information *Nature* thanks Jan Minx, David Reay, Stefan Wirsenius and the other, anonymous, reviewer(s) for their contribution to the peer review of this work.

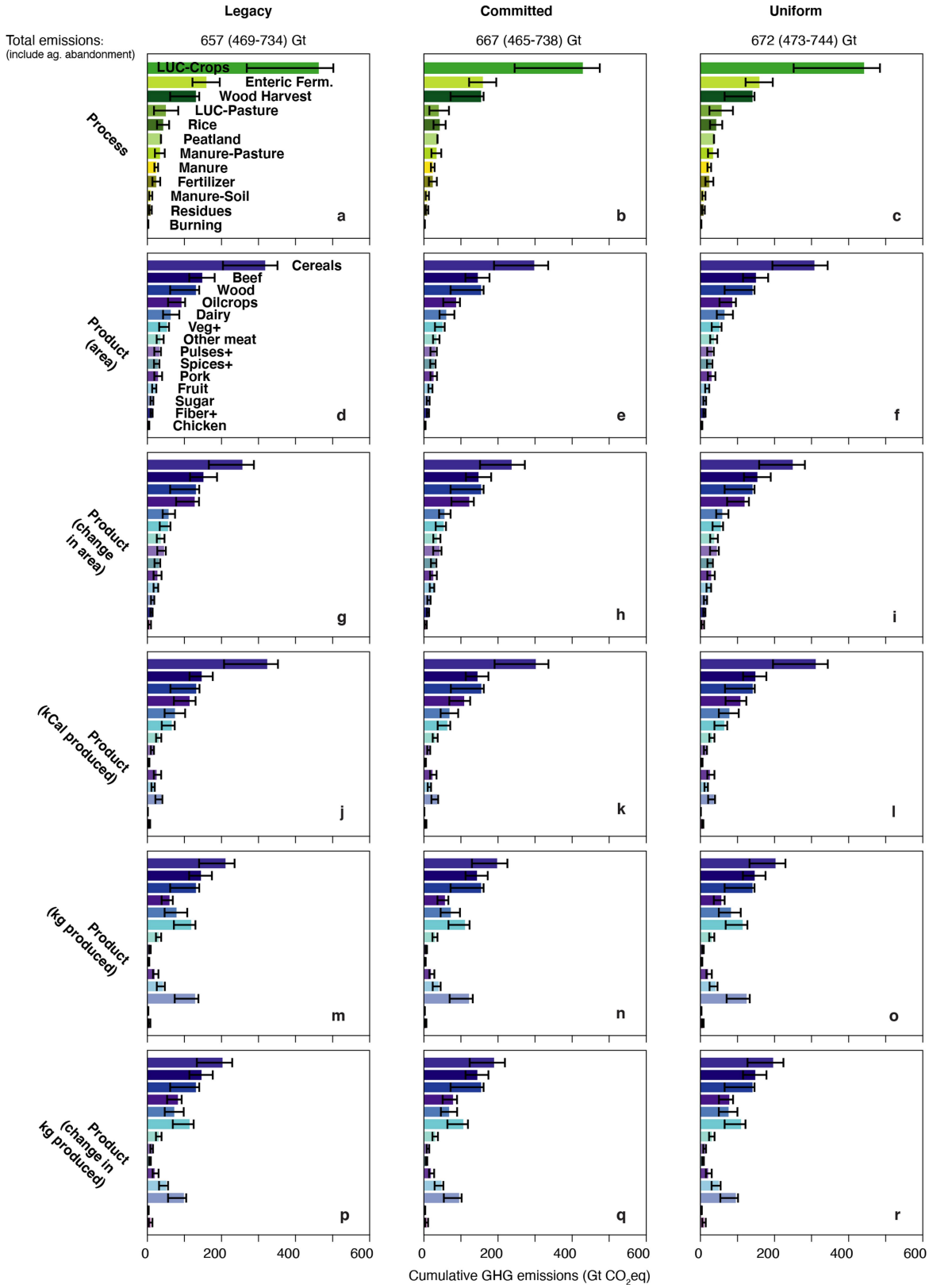

Extended Data Fig. 1 | Differences in global cumulative land-use emissions attributed to processes and products, obtained using different accounting methods. a–**r**, Estimated global cumulative land-use emissions attributed to processes (**a**–**c**) and products (**d**–**r**) over 1961–2017, using different accounting methods to distribute land-use change emissions over time and to products. Our base results (**a**, **d**) reflect emissions occurring in each year owing to past changes in land use (legacy emissions; left), calculated using GWP_{100}, and allocated among crops and livestock by land area used. Different methods to distribute land-use change emissions over time have also been evaluated, that is, all future emissions from a change in land use are assigned to the year of the change (committed emissions; middle) and committed emissions amortized uniformly over 20 years (uniformly distributed emissions; right). Different methods to distribute land-use change emissions to products have also been evaluated, that is, allocating among crops and livestock by change in land area (**g**–**i**), calories of production (**j**–**l**), mass of production (**m**–**o**) and change in mass of production (**p**–**r**) (see Methods). Error bars denote uncertainty ranges (68% intervals), determined by uncertainties in land-use change emissions and in agricultural emissions, as well as uncertainties in the GWP_{100} values. Carbon uptake from agriculture abandonment (negative emissions) is not shown.

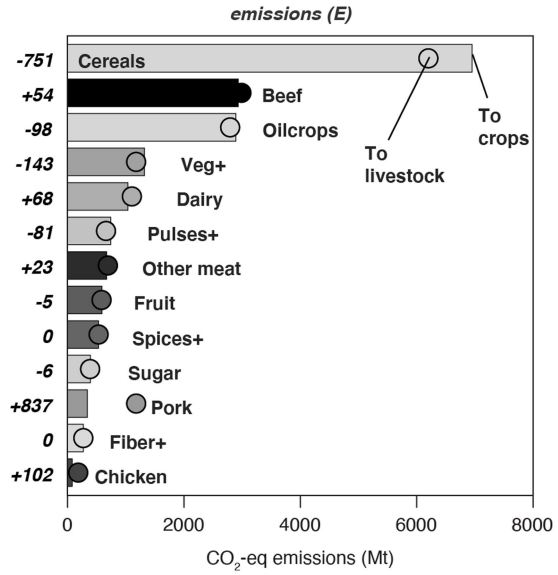

Extended Data Fig. 2 | Global land-use emissions by product group in 2017, with two accountings of the emissions related to feed crops. Our base case allocates the feed crop emissions to the crops themselves (bars). The results of the other accounting—allocating the feed crop emissions to the livestock that consumed the feed—are shown by dots. Numbers are the emissions related to crops fed to livestock (negative values for crops and positive values for livestock) in units of Mt CO_2-eq.

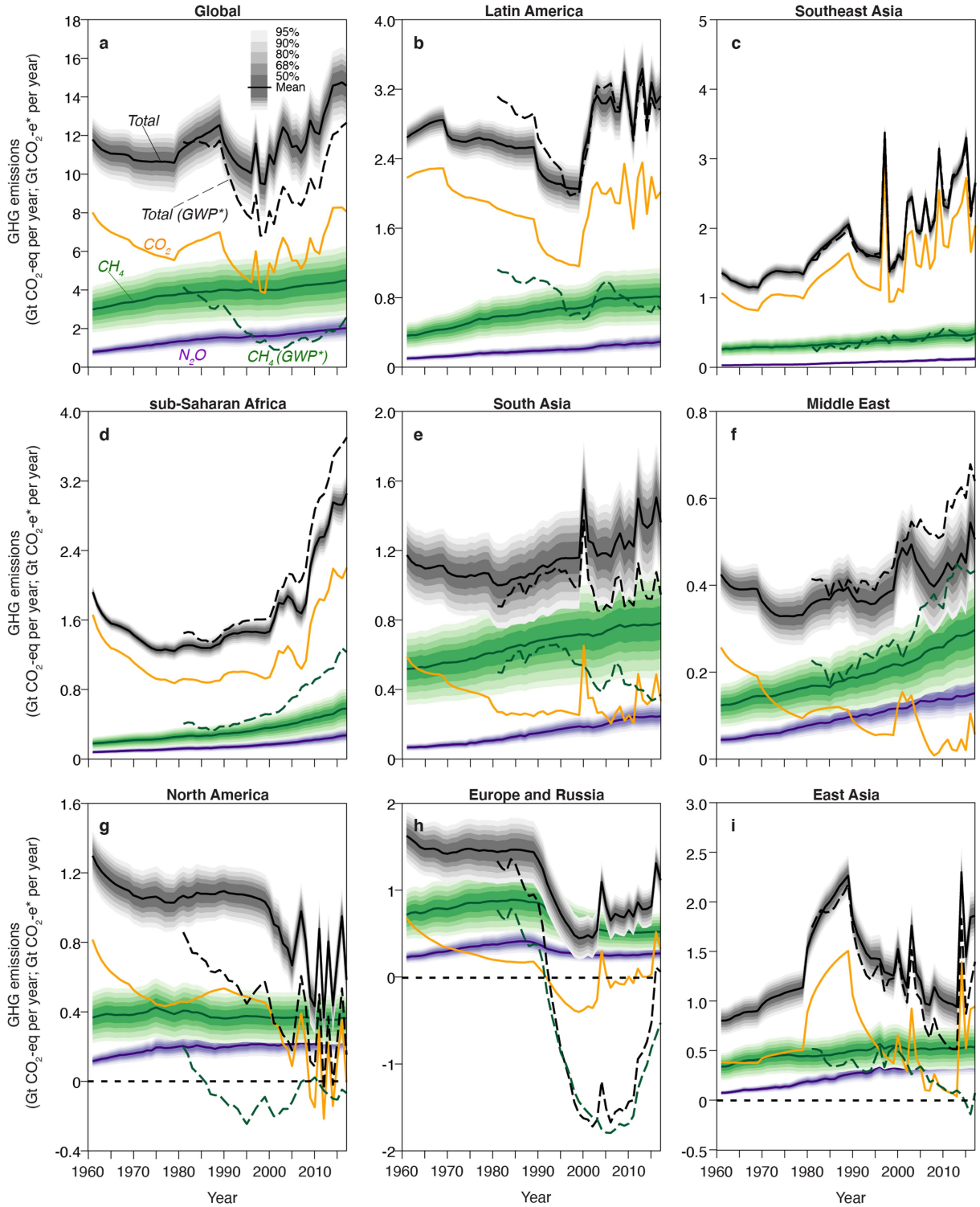

Extended Data Fig. 3 | Uncertainties in global and regional land-use GHG emissions over the period 1961–2017 related to emission metrics. **a**–**i**, Curves show trends in CO_2 (orange), CH_4 (green), N_2O (purple) and total GHG emissions (black) for the global total (**a**) and for each region (**b**–**i**). For our base case, we aggregate all GHG emissions (that is, CO_2, CH_4 and N_2O) in units of CO_2-eq using GWP_{100} values of CH_4 and N_2O. Solid curves show trends in CH_4, N_2O and total GHG emissions calculated using GWP_{100}, with the shading reflecting the range of uncertainty in GWP_{100} values. To assess the sensitivity of the results to metric choices, we also estimate emissions using the GWP* method. Dashed curves show trends in CH_4 and total GHG emissions calculated using GWP* (in units of CO_2-e*). For CO_2 and N_2O, CO_2-eq and CO_2-e* emissions are identical. The length of CO_2-e*emissions records is reduced because interannual variability is smoothed with a 20-year running average.

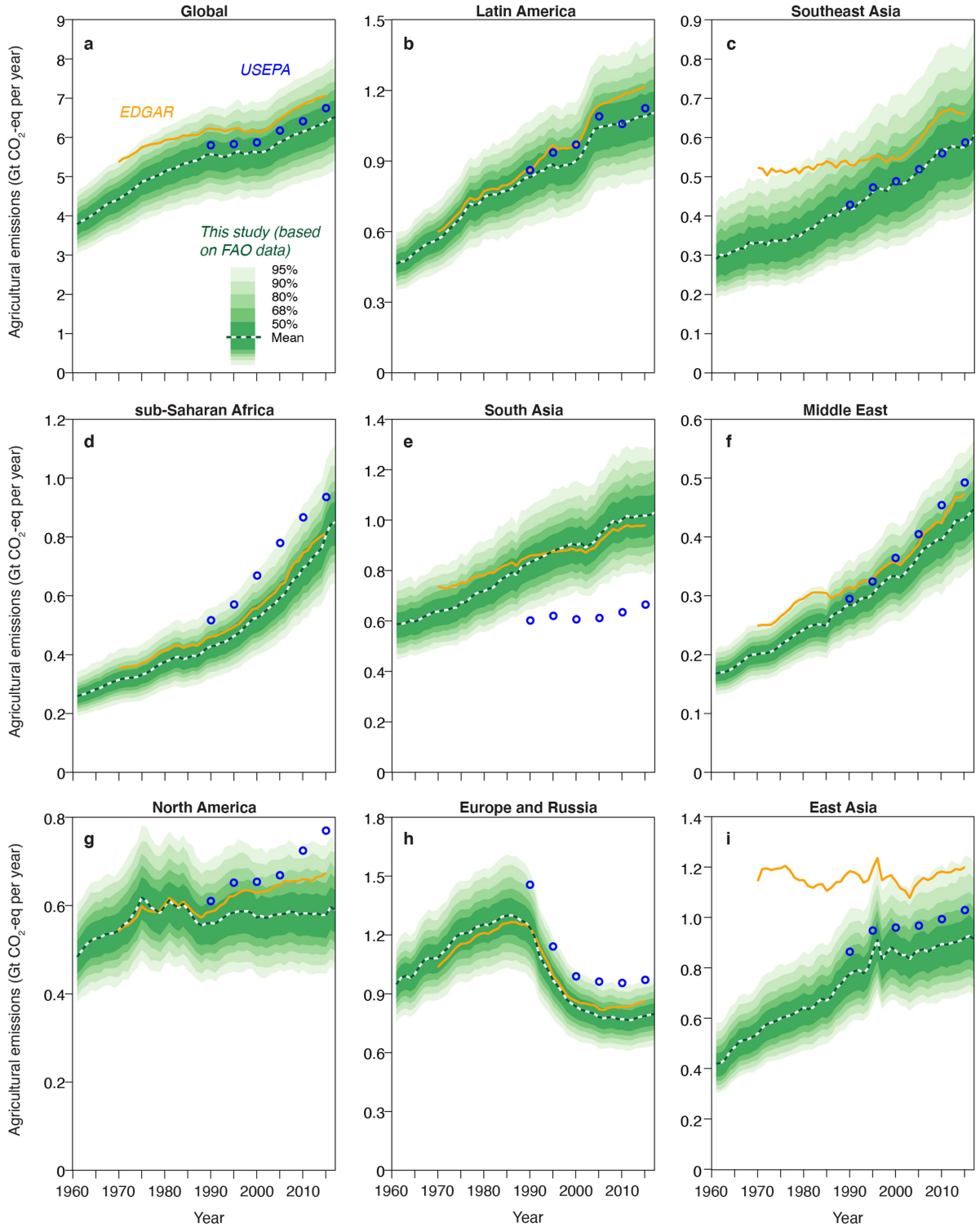

Extended Data Fig. 4 | Comparison of global and regional agricultural emissions between this work, EDGAR and USEPA. a–i, Curves show trends in agricultural emissions for the global total (**a**) and for each region (**b**–**i**), estimated in this work (green; based on FAO data), by EDGAR (orange) and by USEPA (blue). All estimated emissions are converted into CO_2-equivalents, based on the same GWP_{100} values from the IPCC Fifth Assessment Report (34 for CH_4 and 298 for N_2O). The shaded areas reflect the range of uncertainty in agricultural emissions in this work, determined by Monte Carlo analysis (performed by varying activity data, parameter values and emission factors from those used in the FAO database).

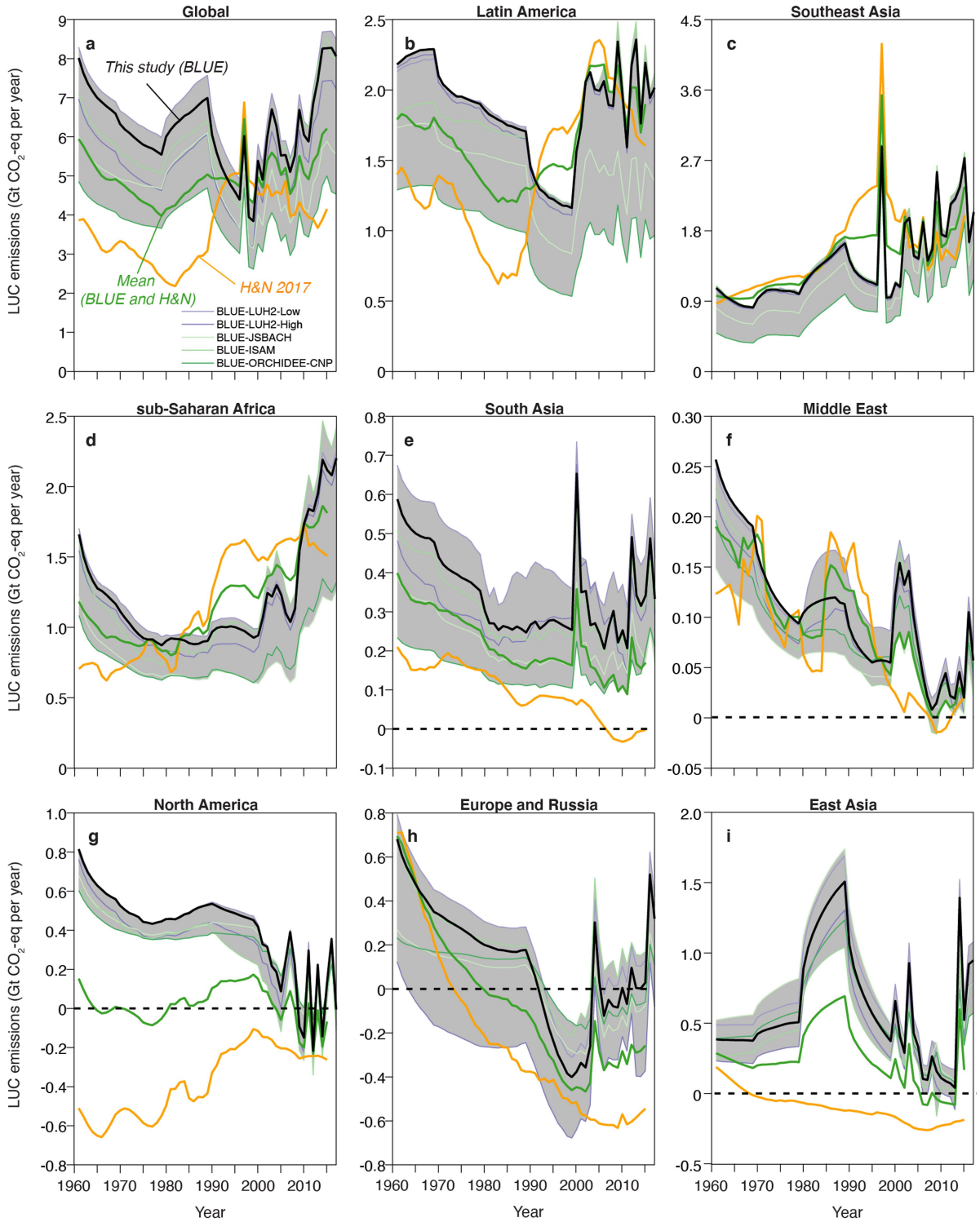

Extended Data Fig. 5 | Comparison of global and regional land-use change emissions between two bookkeeping models. a–i, Curves show trends in land-use change emissions for the global total (**a**) and for each region (**b**–**i**), estimated by BLUE (black; used in this work) and H&N (orange; available until 2015 only). The average of the bookkeeping models (green line) is also shown. The range from the uncertainty simulations with BLUE is shown as the 68% uncertainty range of our estimates (grey areas), with the five additional simulations using different assumptions indicated by thin lines: different assumptions on land-use transitions (purple) and different assumptions on carbon values (green).

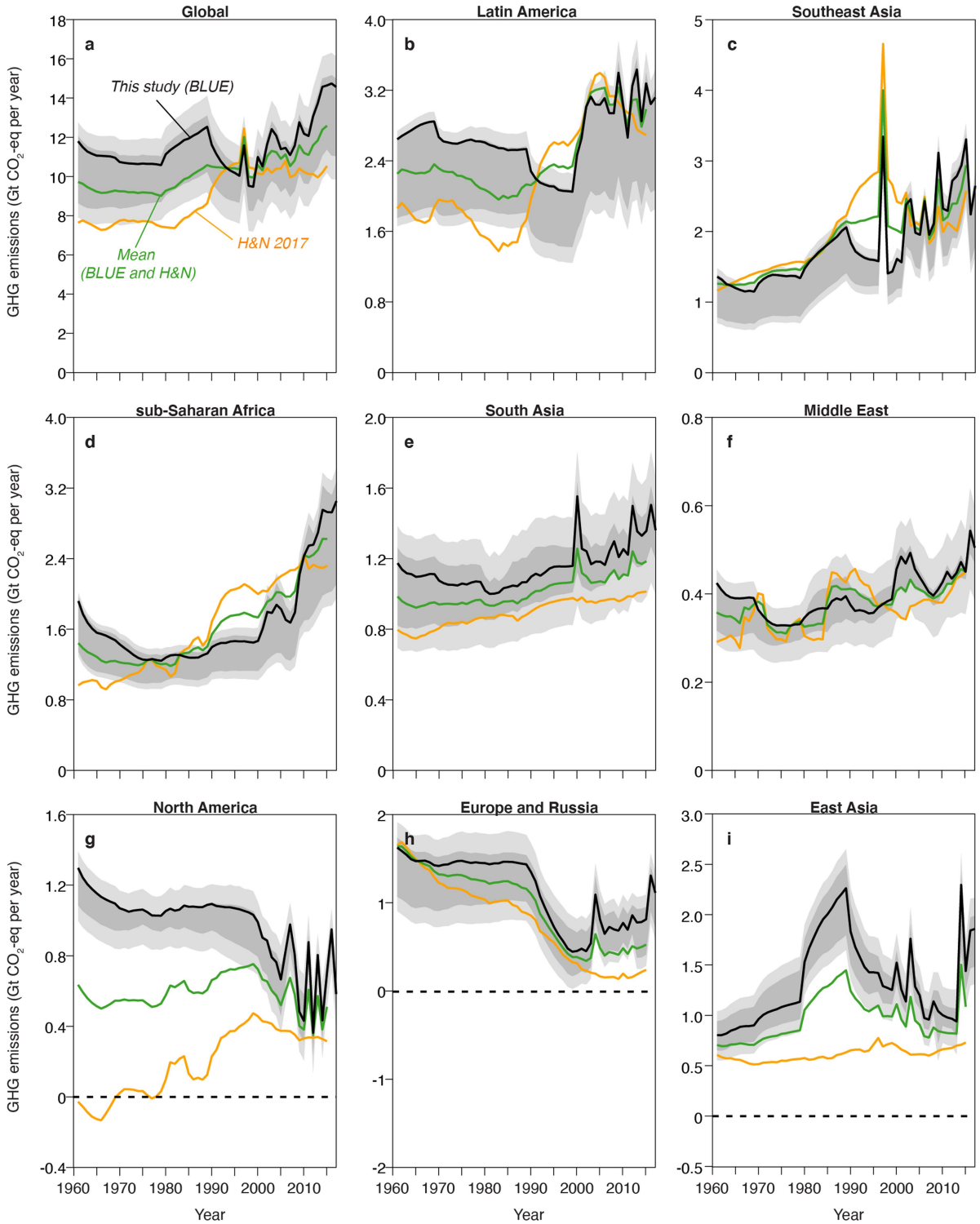

Extended Data Fig. 6 | Comparison of global and regional land-use emissions, obtained using different land-use change emissions from two bookkeeping models. a–i, Curves show trends in land-use emissions for the global total (**a**) and for each region (**b**–**i**), obtained using land-use change emissions from BLUE (black; used in this work) and H&N (orange; available until 2015 only). The average of the two bookkeeping models (green line) is also shown. In this work, we combined agricultural emissions from the FAO with land-use change emissions estimated by the BLUE model to calculate total land-use emissions. We performed sensitivity analyses by also combining the agricultural emissions from the FAO with the land-use change emissions estimated by another bookkeeping model (H&N) and with the average of two bookkeeping models (BLUE and H&N). Lighter grey areas represent uncertainty ranges (68% intervals) of our estimates, determined by uncertainties in land-use change emissions and in agricultural emissions, as well as uncertainties in the GWP_{100} values. Darker grey areas show uncertainties only related to land-use change emissions, determined from additional simulations with the BLUE model.

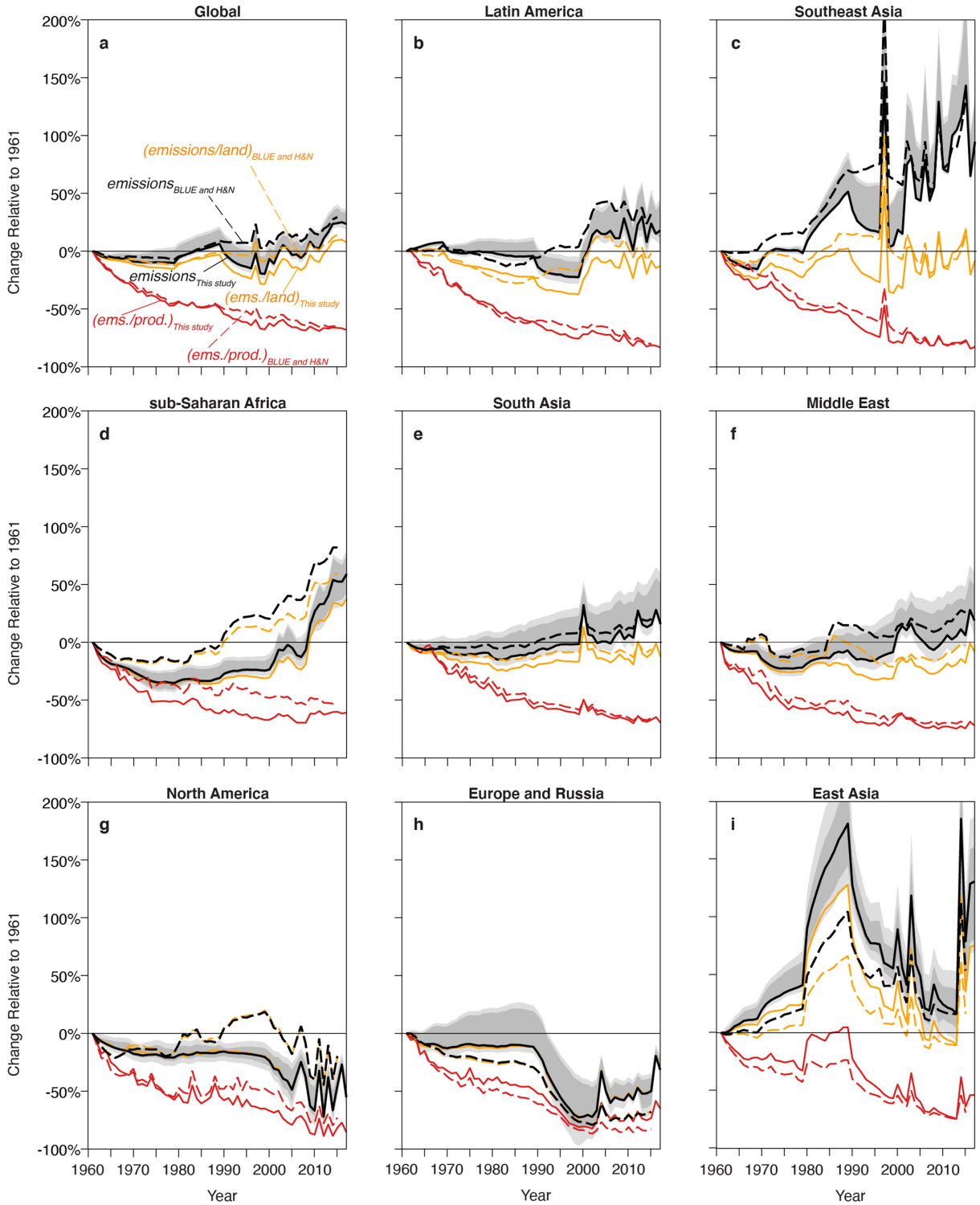

Extended Data Fig. 7 | Comparison of global and regional trends in land-use emissions and *Pale* factors, obtained using different land-use change emission inventories. a–i, Curves show trends in land-use emissions (black), emissions intensity of land use (orange) and agricultural production (red) for the global total (**a**) and for each region (**b**–**i**), using land-use change emissions from BLUE (solid lines; used in this work) and the combination of two bookkeeping models (dashed lines; available until 2015 only). In this work, we combined agricultural emissions from the FAO with land-use change emissions estimated by the BLUE model to perform *Pale* analysis of land-use emissions. We also performed an additional *Pale* analysis by using agricultural emissions from the FAO combined with the average of land-use change emissions from two bookkeeping models (BLUE and H&N). Lighter grey areas represent uncertainty ranges (68% intervals) of our estimates, determined by uncertainties in land-use change emissions and in agricultural emissions, as well as uncertainties in the GWP_{100} values. Darker grey areas show uncertainties related only to land-use change emissions, determined from additional simulations with the BLUE model.

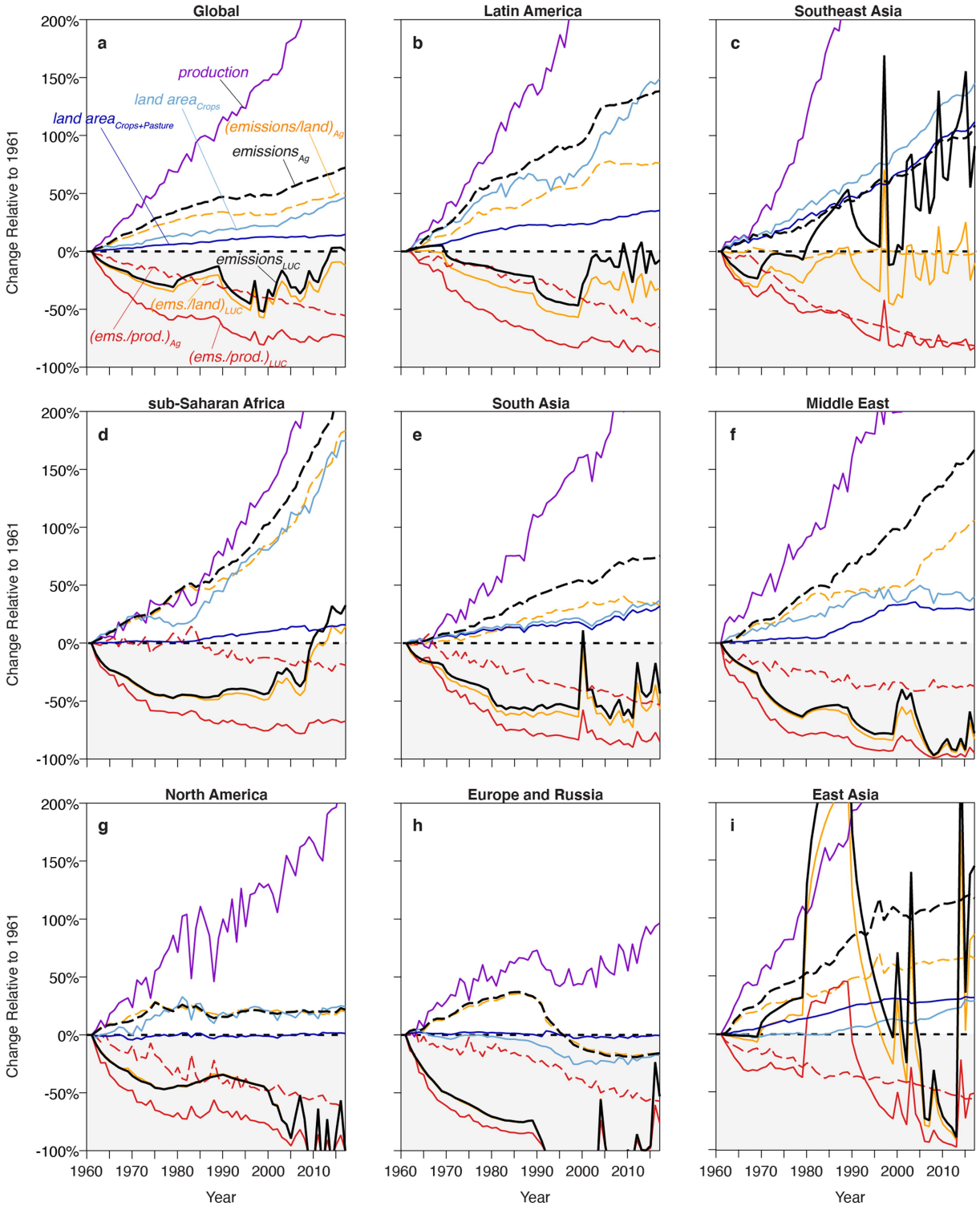

Extended Data Fig. 8 | Global and regional trends in *Pale* factors contributing to land-use emissions during 1961–2017, decomposed into land-use change emissions and agricultural emissions. a–i, Curves show changes in the *Pale* factors contributing to land-use change (LUC, solid lines) emissions and agricultural (Ag, dashed lines) emissions over the period 1961–2017 for the global total (**a**) and for each region (**b**–**i**) relative to 1961. Results shown are for our base assumptions (see Extended Data Fig. 1), and different curves are labelled in **a**. Oceania is not shown.

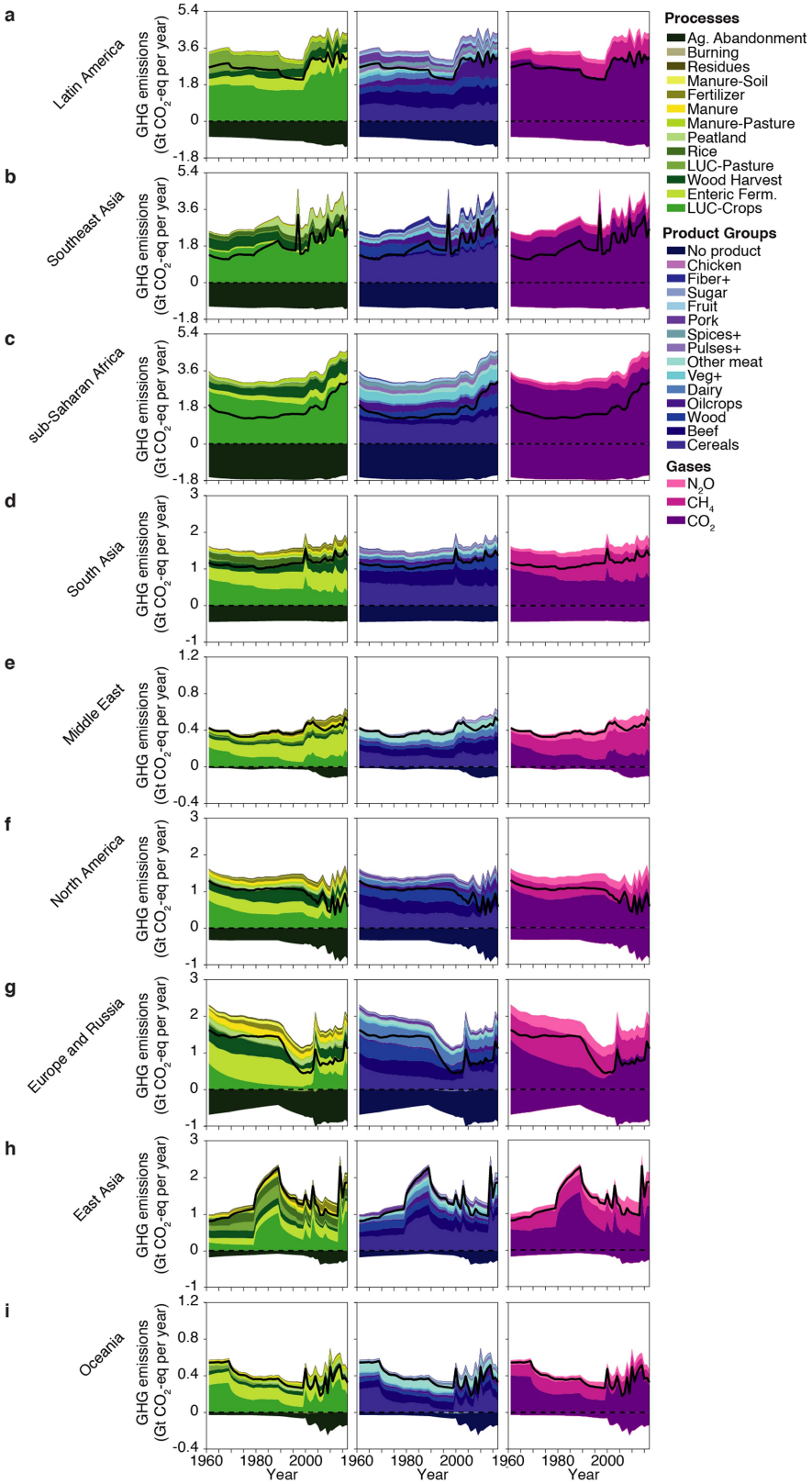

Extended Data Fig. 9 | Estimated land-use emissions over the period 1961–2017 for nine world regions. a–i, Estimated land-use emissions for each region (**a**–**i**) by process, product group and GHG emitted. In each panel, net emissions are shown by the bold black line.

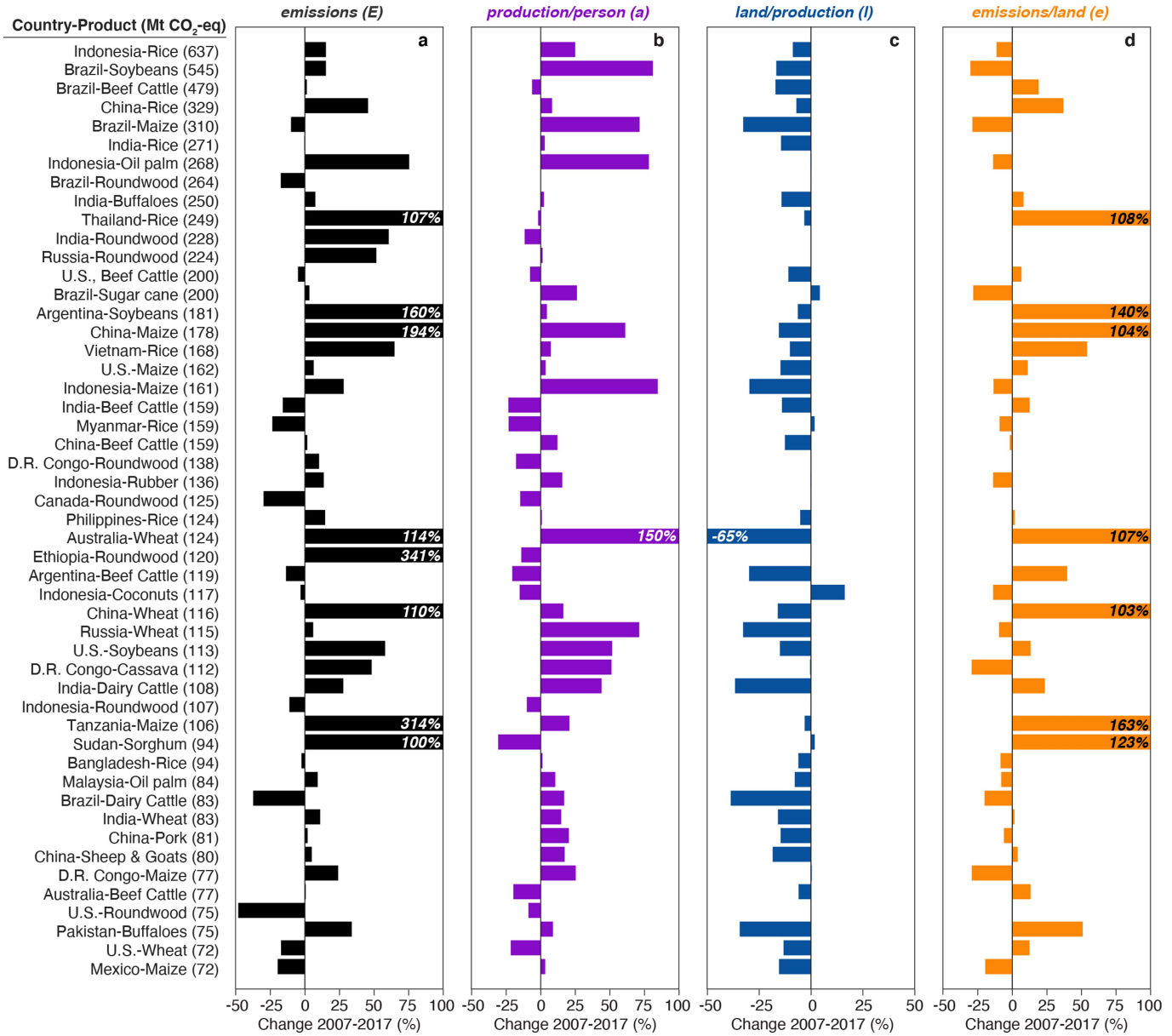

Extended Data Fig. 10 | Changes in 2007–2017 in *Pale* factors of the 50 country–product sources with the largest annual emissions. a–d, Bars show the per cent change in annual land-use emissions (**a**), per capita production (**b**), land intensity of production (**c**) and emissions intensity of land use (**d**) for each country–product combination.

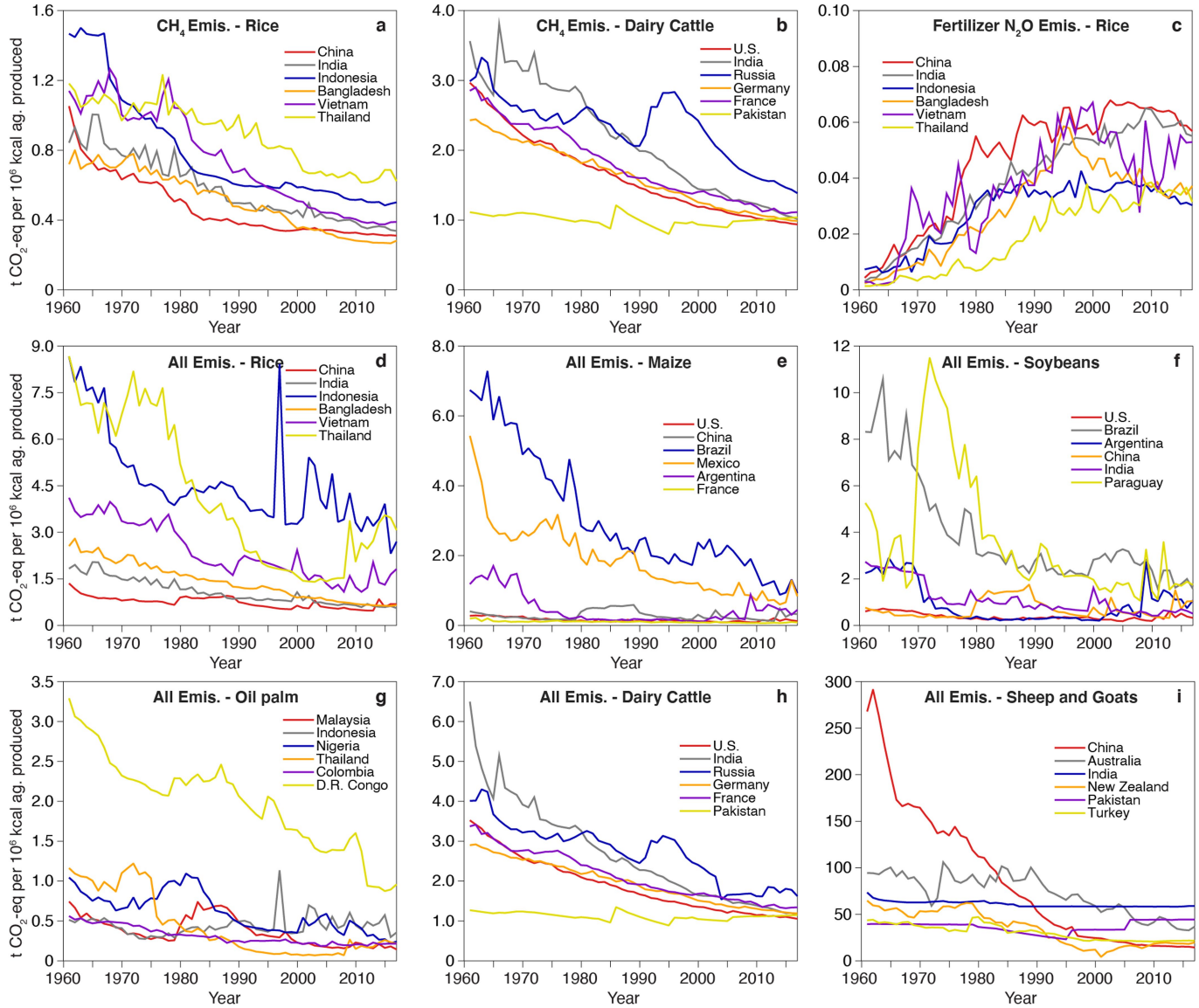

Extended Data Fig. 11 | Trends in emissions intensity of major agricultural products. a–c, Curves show trends in emissions intensity of processes including CH_4 emissions from rice (**a**) and dairy cattle (**b**) production and N_2O emissions from fertilizer use for rice production (**c**). **d–i**, Curves show trends in emissions intensity of major agricultural products including rice (**d**), maize (**e**), soybeans (**f**), oil palm (**g**), dairy cattle (**h**) and sheep and goats (**i**). Total emissions per calorie of agricultural production (**d–i**) in the six countries that produce the most of each product tend to decrease over time, but in all cases remain greater than zero.

Extended Data Table 1 | Data sources used for the study

Data	Temporal Resolution	Spatial Resolution	Units	Sectoral/Activity Resolution	Source
Historical land use	Annual	0.5˚ x 0.5˚	% yr^{-1} $cell^{-1}$	5 land uses	Hurtt et al. (2020)[51]
Land-use change (LUC) emissions	Annual	0.5˚ x 0.5˚	t yr^{-1} $cell^{-1}$	1 GHG (CO_2); 5 processes (LUC-Crops, LUC-Pasture, ag. abandonment, wood harvest, peatland emissions)	Hansis et al. (2015)[24]; FAO (2019)[15]; GFED4s (2017)[57]
Agricultural emissions	Annual	Country-level	t yr^{-1}	2 GHGs (CH_4, N_2O); 8 processes (enteric fermentation, rice cultivation, fertilizer, manure management, manure applied to soils, manure left on pasture, agricultural residues, burning); 161 crops; 7 livestock types	FAO (2019)[15]
Crops and livestock produced	Annual	Country-level	t yr^{-1}	161 crops; 7 livestock types	FAO (2019)[15]
Forest products produced	Annual	Country-level	m^3 yr^{-1}	1 product	FAO (2019)[15]
Cropland harvested and pasture area	Annual	Country-level	hectare yr^{-1}	161 crops; no livestock type	FAO (2019)[15]
Livestock densities	Annual	0.05˚ x 0.05˚	head yr^{-1} km^{-2}; birds yr^{-1} km^{-2}	6 livestock types	Robinson et al. (2007, 2014)[67,68]

Data from refs. [15,24,51,57,67,68].

Extended Data Table 2 | 169 agricultural products and their categorization

Product Name	Group	Product Name	Group	Product Name	Group
Agave fibres nes	Fiber+	Fruit- tropical fresh nes	Fruit	Popcorn	Cereals
Almonds- with shell	Pulses+	Garlic	Veg+	Poppy seed	Oilcrops
Anise- badian- fennel- coriander	Spices+	Ginger	Spices+	Potatoes	Veg+
Apples	Fruit	Gooseberries	Fruit	Pulses- nes	Pulses+
Apricots	Fruit	Grain- mixed	Cereals	Pumpkins- squash and gourds	Veg+
Areca nuts	Spices+	Grapefruit (inc. pomelos)	Fruit	Pyrethrum- dried	Spices+
Artichokes	Veg+	Grapes	Fruit	Quinces	Fruit
Asparagus	Veg+	Groundnuts- with shell	Oilcrops	Quinoa	Cereals
Avocados	Fruit	Hazelnuts- with shell	Pulses+	Ramie	Fiber+
Bambara beans	Pulses+	Hemp tow waste	Fiber+	Rapeseed	Oilcrops
Bananas	Fruit	Hempseed	Oilcrops	Raspberries	Fruit
Barley	Cereals	Hops	Spices+	Rice- paddy	Cereals
Bastfibres- other	Fiber+	Jojoba seed	Oilcrops	Roots and tubers- nes	Veg+
Beans- dry	Pulses+	Jute	Fiber+	Rubber- natural	Fiber+
Beans- green	Veg+	Kapok fruit	Fiber+	Rye	Cereals
Berries nes	Fruit	Karite nuts (sheanuts)	Oilcrops	Safflower seed	Oilcrops
Blueberries	Fruit	Kiwi fruit	Fruit	Seed cotton	Oilcrops
Brazil nuts- with shell	Pulses+	Kola nuts	Spices+	Sesame seed	Oilcrops
Broad beans- horse beans- dry	Pulses+	Leeks- other alliaceous vegetables	Veg+	Sisal	Fiber+
Buckwheat	Cereals	Lemons and limes	Fruit	Sorghum	Cereals
Cabbages and other brassicas	Veg+	Lentils	Pulses+	Soybeans	Oilcrops
Canary seed	Cereals	Lettuce and chicory	Veg+	Spices- nes	Spices+
Carobs	Fruit	Linseed	Oilcrops	Spinach	Veg+
Carrots and turnips	Veg+	Lupins	Pulses+	Strawberries	Fruit
Cashew nuts- with shell	Pulses+	Maize- green	Veg+	String beans	Veg+
Cashewapple	Fruit	Maize	Cereals	Sugar beet	Sugar
Cassava leaves	Veg+	Mangoes- mangosteens- guavas	Fruit	Sugar cane	Sugar
Cassava	Veg+	Manila fibre (abaca)	Fiber+	Sugar crops- nes	Sugar
Castor oil seed	Oilcrops	Mat	Spices+	Sunflower seed	Oilcrops
Cauliflowers and broccoli	Veg+	Melons- other (inc.cantaloupes)	Veg+	Sweet potatoes	Veg+
Cereals- nes	Cereals	Melonseed	Oilcrops	Tallowtree seed	Oilcrops
Cherries- sour	Fruit	Millet	Cereals	Tangerines- mandarins- clementines- satsumas	Fruit
Cherries	Fruit	Mushrooms and truffles	Veg+	Taro (cocoyam)	Veg+
Chestnut	Pulses+	Mustard seed	Oilcrops	Tea	Spices+
Chick peas	Pulses+	Nutmeg- mace and cardamoms	Spices+	Tobacco- unmanufactured	Spices+
Chicory roots	Spices+	Nuts- nes	Pulses+	Tomatoes	Veg+
Chillies and peppers- dry	Spices+	Oats	Cereals	Triticale	Cereals
Chillies and peppers- green	Veg+	Oil palm fruit	Oilcrops	Tung nuts	Oilcrops
Cinnamon (canella)	Spices+	Oilseeds nes	Oilcrops	Vanilla	Spices+
Cloves	Spices+	Okra	Veg+	Vegetables- fresh nes	Veg+
Cocoa- beans	Spices+	Olives	Oilcrops	Vegetables- leguminous nes	Veg+
Coconuts	Oilcrops	Onions- dry	Veg+	Vetches	Pulses+
Coffee- green	Spices+	Onions- shallots- green	Veg+	Walnuts- with shell	Pulses+
Cow peas- dry	Pulses+	Oranges	Fruit	Watermelons	Veg+
Cranberries	Fruit	Papayas	Fruit	Wheat	Cereals
Cucumbers and gherkins	Veg+	Peaches and nectarines	Fruit	Yams	Veg+
Currants	Fruit	Pears	Fruit	Yautia (cocoyam)	Veg+
Dates	Fruit	Peas- dry	Pulses+	Chickens- layers	Dairy
Eggplants (aubergines)	Veg+	Peas- green	Veg+	Chickens- broilers	Chicken
Fibre crops nes	Fiber+	Pepper (piper spp.)	Spices+	Cattle- dairy	Dairy
Figs	Fruit	Peppermint	Spices+	Sheep and Goats	Other meat
Flax fibre and tow	Fiber+	Persimmons	Fruit	Cattle- non-dairy	Beef
Fonio	Cereals	Pigeon peas	Pulses+	Buffaloes	Beef
Fruit- citrus nes	Fruit	Pineapples	Fruit	Swine	Pork
Fruit- fresh nes	Fruit	Pistachios	Pulses+	Roundwood	Wood
Fruit- pome nes	Fruit	Plantains and others	Fruit		
Fruit- stone nes	Fruit	Plums and sloes	Fruit		

nes, not elsewhere specified.